

New Applications of Spectroscopic Methods in Biomedical and Pharmaceutical Analysis : A Survey

ERIC J. LIEN AND HUA GAO

*Department of Pharmaceutical Sciences
School of Pharmacy, University of Southern California
1985 Zonal Ave., LA, CA 90033*

ABSTRACT

In recent years various fields of spectroscopy have been developed into powerful tools of qualitative and quantitative analyses in biomedical and pharmaceutical research and development. These include IR, NMR, UV-visible spectroscopy and X-ray spectrography in molecular structure determination. In this survey the underlying principles and selected examples of these applications will be presented, including the fundamental equations for IR, NMR, the physical properties of common nuclei of biomedical interest (^1H , ^2H , ^{13}C , ^{15}N , ^{19}F and ^{31}P), the use of FT-IR with ^{13}C and ^{15}N labeling for studying protein-protein interactions, FT-IR study of the effects of cholesterol on conformational disorder in lipid bilayers, pKa determination of N-hydroxy-N'-aminoquanidine derivatives by ^{15}N -NMR, ^{19}F -MR quantitation of lens aldose reductase activity using 3-deoxy-3-F-D-glucose, ^{31}P -NMR evaluation of postischemia renal ATP and pH levels after ATP-MgCl₂ treatment in rabbits, solid-state NMR in the analysis of polymorphism, applications of 2D-NMR in structural determination (e.g. COSY, DQFCOSY, NOESY, HMBC, HMQC, and 2D-INADEQUATE), and analysis of flucytosine dosage forms by derivative UV spectroscopy.

It is hoped that this survey will stimulate the ever increasing applications of spectroscopic methods in solving complex biomedical and pharmaceutical problems.

Key words : UV-visible, X-ray, IR, 2D-NMR and Solid-state NMR

INTRODUCTION

The electromagnetic wave spectrum of the range from 1 Å (10^{-8}cm) to over 25 cm covers a wide range of subatomic, atomic and molecular transitions, vibration, and rotations utilized in the development of various forms of spectrometry in recent years⁽¹⁾ (see Figure.1). Among

these, UV-visible, IR, NMR spectrometry and X-ray spectrography are most commonly used in molecular structure determination in biomedical and pharmaceutical research and development⁽¹⁾ (see Figure.2 for details).

In order to fully comprehend the utilizations and limitations of various forms of instrumentation, it is necessary to understand the underlying principles involved. The fundamental

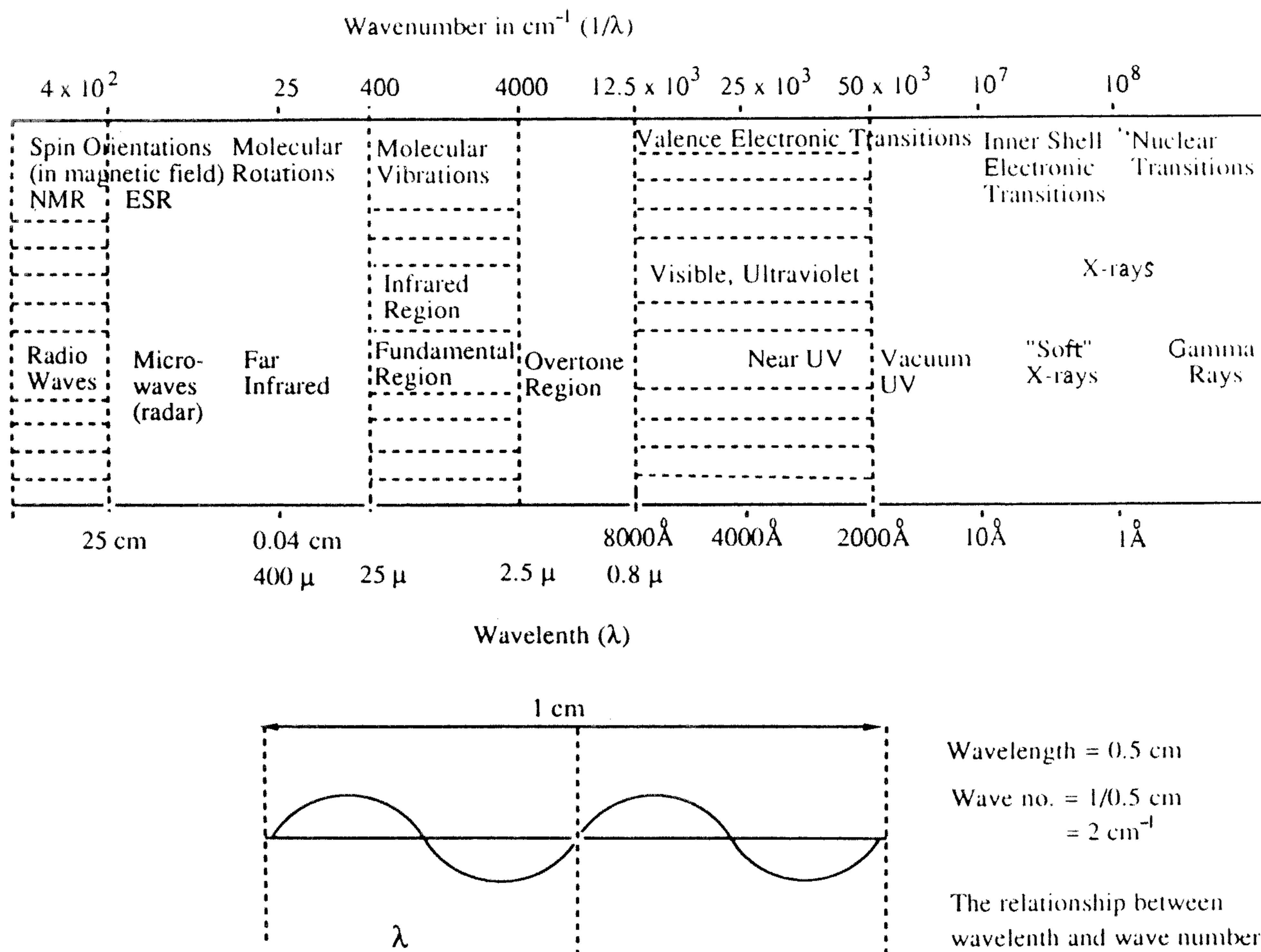


Figure 1. Schematic diagram of electromagnetic spectrum and various forms of spectrometry used in pharmaceutical and biomedical analysis. Shaded areas represent the most commonly used regions. (Adapted from R.T. Bauman, Absorption Spectroscopy, 1962, p.11)

equations for UV-visible, IR and NMR spectrometry will be briefly reviewed and selected applications of them will be presented.

UN-VISIBLE SPECTROMETRY

The molecular absorption of energy in the UV-visible region is dependent on the valence electronic transition. It is most commonly used in the quantitative analysis of compounds with chromophore (which is a covalently unsaturated group responsible for absorption) and auxochrome, a saturated group which alters both the wavelength (λ_{max}), and the intensity of the absorption maximum (ϵ_{max}). The fundamental equation

governing the relationship between the absorbance (A) and the molar absorptivity (ϵ), the concentration (c , moles/liter) and the path length (b) is known as the Lambert-Beer Law⁽²⁾.

$$A = \epsilon \cdot c \cdot b \quad (1)$$

Various transitions involving different electronic structures (σ , n , π) occur at different λ_{max} with different ϵ_{max} values. Figure 3 and Figure 4 show the UV absorption spectra of cyclic thioureas in three different solvents. It is worth noting that the different solvents affect not only the λ_{max} but also ϵ_{max} ⁽²⁾. In Figures 3 and 4 one can see that as the polarity of the solvents is increased from n-heptane to ethanol and water, there is a

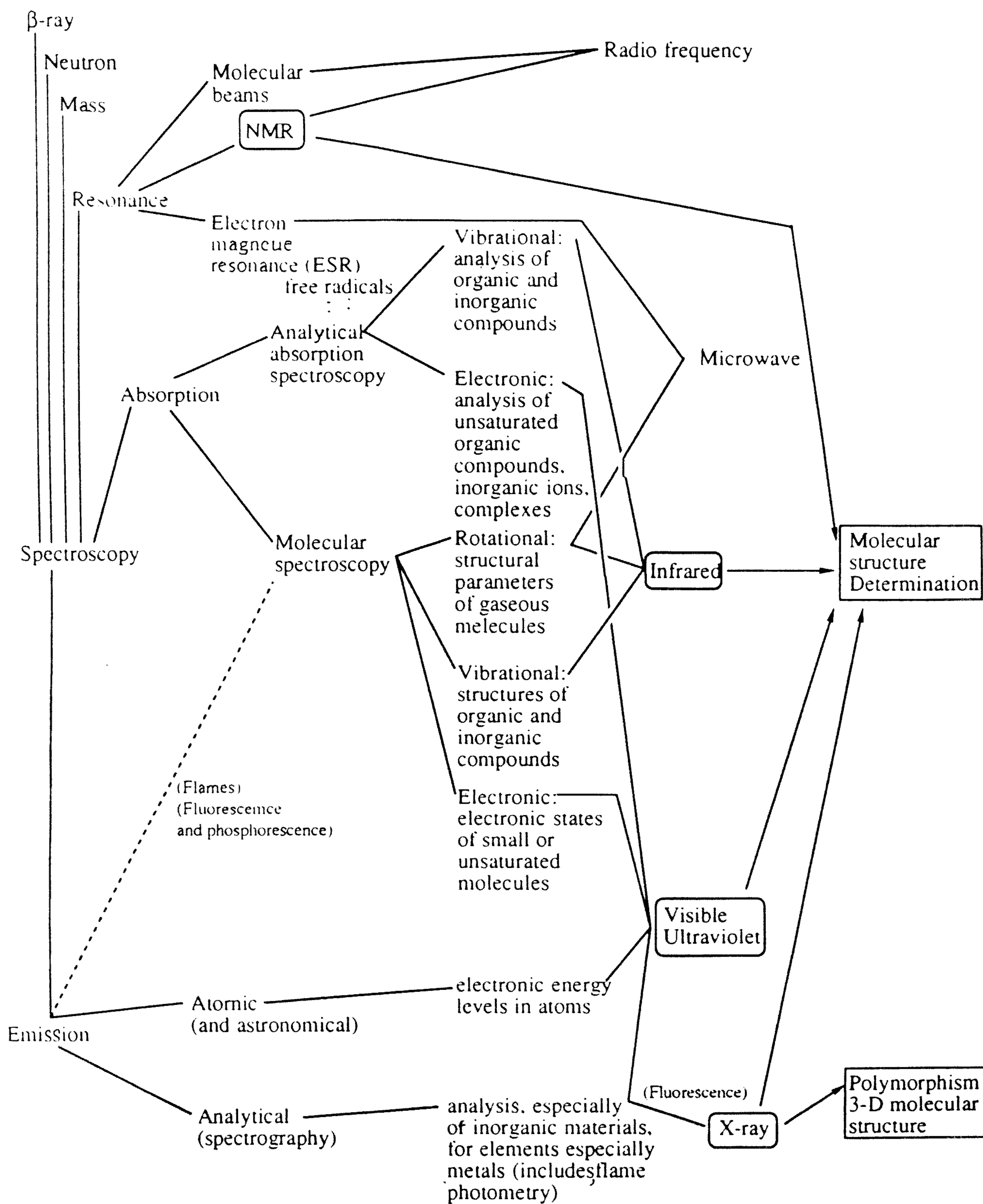


Figure 2. Various Fields of spectroscopy and their applications in molecular structure determination. (Adapted from R.T. Bauman, Absorption Spectroscopy, 1962, p.13)

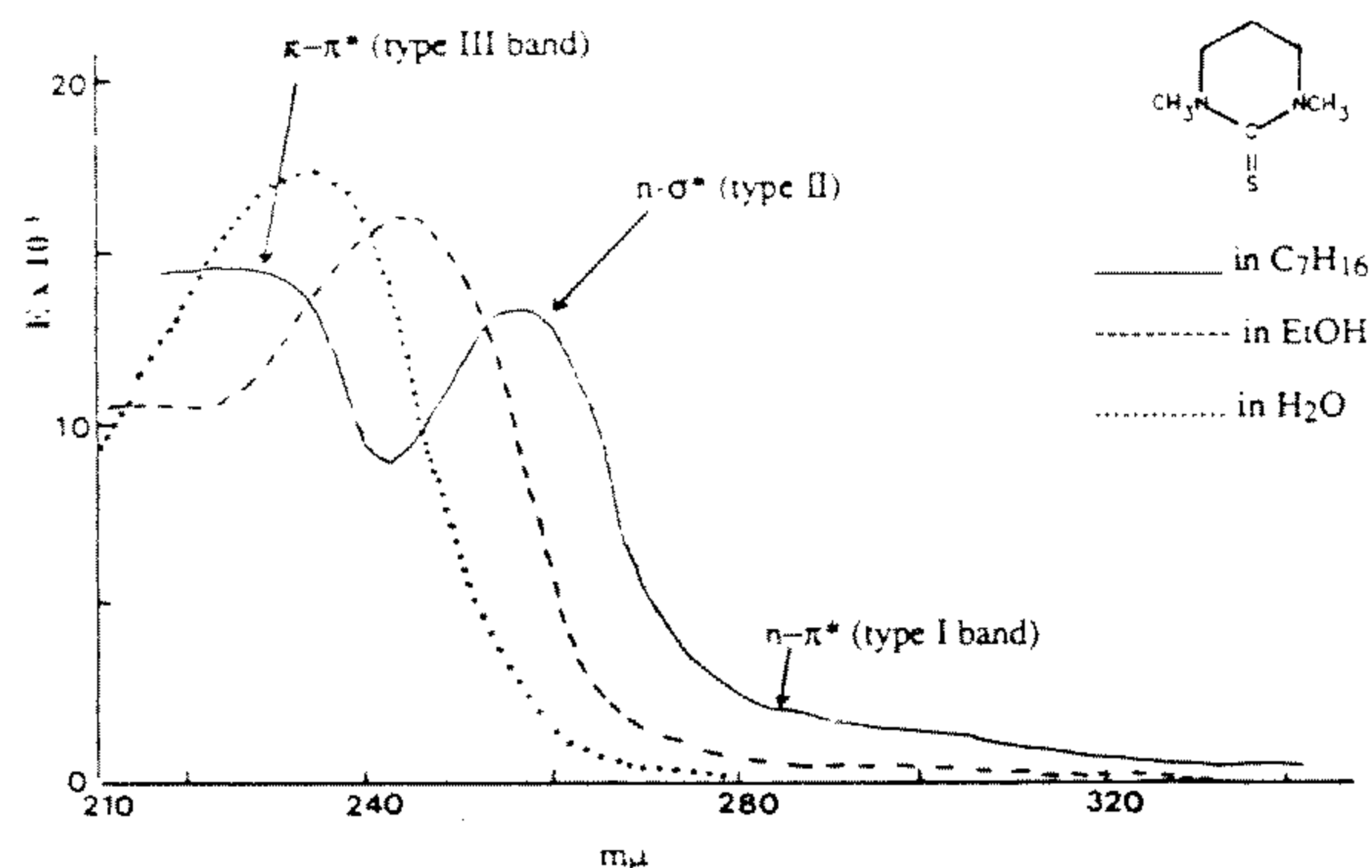


Figure 3. The UV spectra of N,N'-dimethyltri-methylenethiourea.

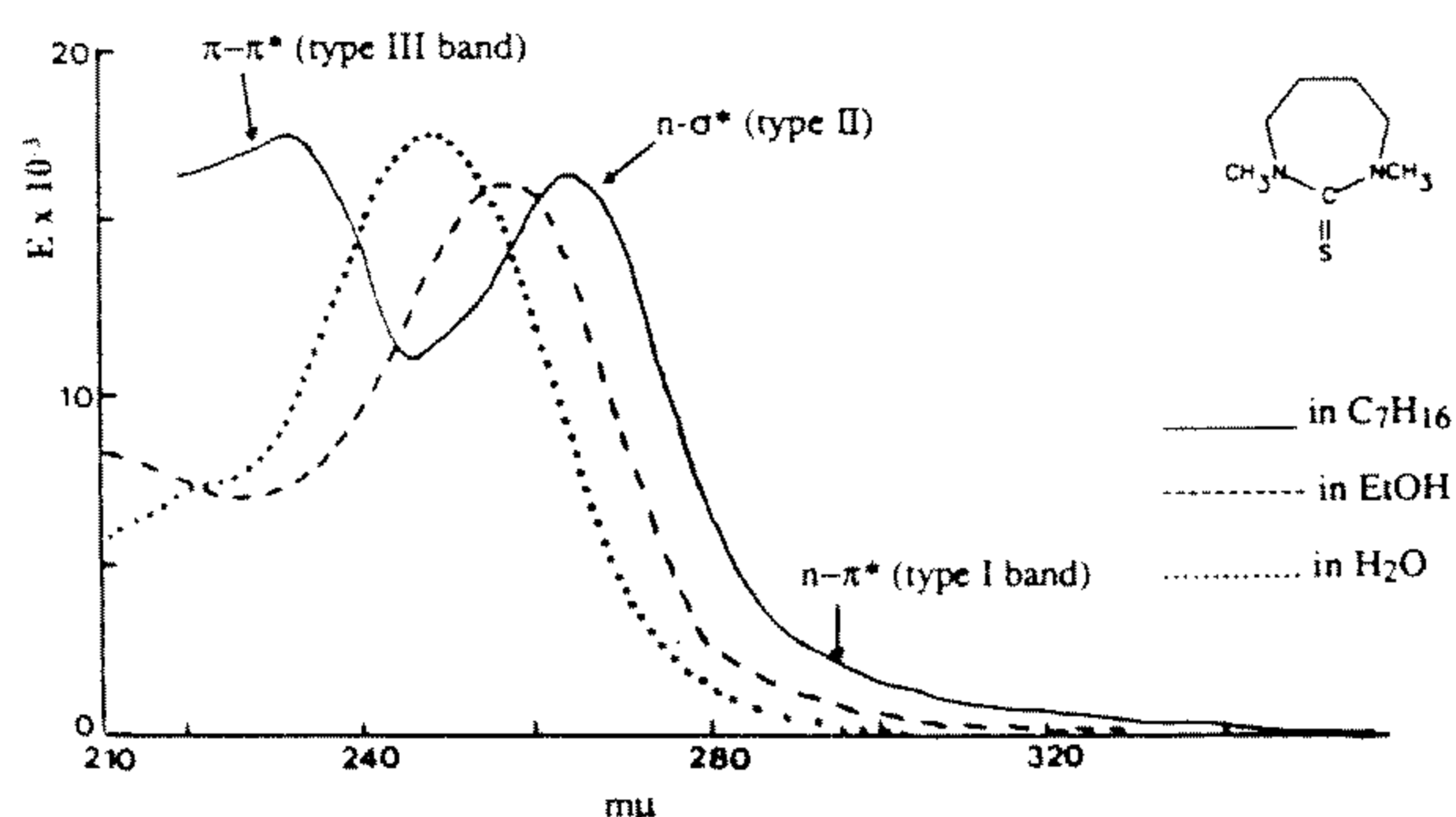


Figure 4. The UV spectra of N,N'-dimethyltetra-methylenethiourea.

gradual blue (hypsochromic) shift of the $n-\sigma^*$ and $n-\pi^*$ (types II and I) transition, due to hydrogen bonding of the lone pair electrons with EtOH and H₂O, and more energy (shorter wavelength) is required for the transition. For type III ($\pi-\pi^*$) band a red (bathochromic) shift is observed by increasing the polarity of the solvent, resulting from an electron redistribution with enhanced electron density in the peripheral parts of the molecule where the electrons are more accessible for H-bond formation⁽³⁾.

In recent years first derivative spectrophotometry⁽⁴⁾ has received increasing attention in the assay of drug formulations in clinical and biological applications and in determination of degradation products⁽⁴⁻⁶⁾. It involves the plot of first derivative $D_1 = dA/d\lambda$ as a function of wavelength (λ). The method has been successfully applied to the determination of propranolol in inderal tablets⁽⁵⁾, fluorometholone

and neomycin sulfate in combination⁽⁶⁾ and many others⁽⁴⁾. An excellent review article by Lee is available on the applications of first, second and higher order derivative spectroscopy in drug analysis⁽⁴⁾.

Cavrini et al. have successfully applied derivative UV spectroscopy to the quality control of commercial dosage forms of flucytosine and the results have been compared with those obtained by a HPLC procedure developed as a reference method.⁽⁷⁾

FUNDAMENTAL EQUATIONS FOR IR SPECTROSCOPY AND APPLICATIONS

The necessary and sufficient condition for IR absorption by a molecule is that a certain molecular vibration leads to a change in molecular electric dipole moment. The energy absorbed is related to the frequency of the electromagnetic wave (ν) by the equation:

$$E = h\nu \quad (2)$$

where h is the plank's constant and ν is related to the reduced mass of two atoms with mass of m_1 and m_2 respectively :

$$\nu = \frac{1}{2\pi c} \sqrt{\frac{f}{\mu}} \quad (3)$$

where c = velocity of light (cm/sec)

$\mu = m_1 \cdot m_2 / (m_1 + m_2)$

f = force constant (dynes/cm)

Using this equation, one can calculate that the f for single bonds will be around 5×10^5 dynes/cm, and 10 to 15×10^5 dynes/cm for double and triple bonds, respectively, the exact number depends on the type of atoms connected and the rest of the molecule.

IR spectroscopy is most useful in the qualitative detection and identification of functional groups and specific molecular structures. It can also be used to detect either intra- or in-

Table 1. The IR stretching frequency of exocyclic double bond as a function of the ring strain⁽³⁾

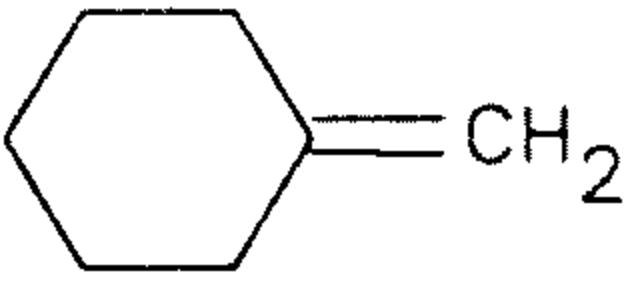
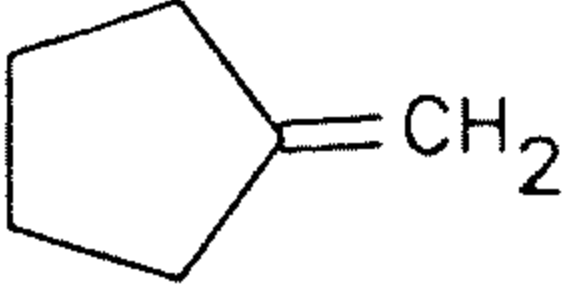
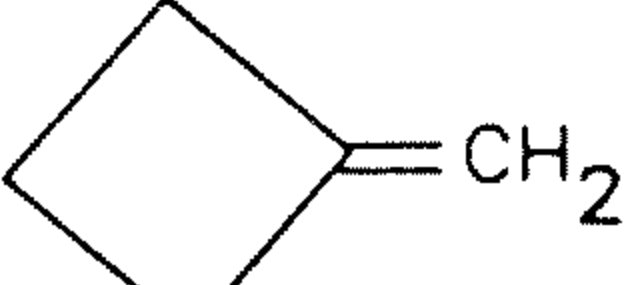
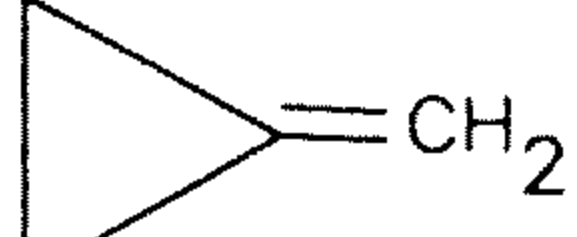
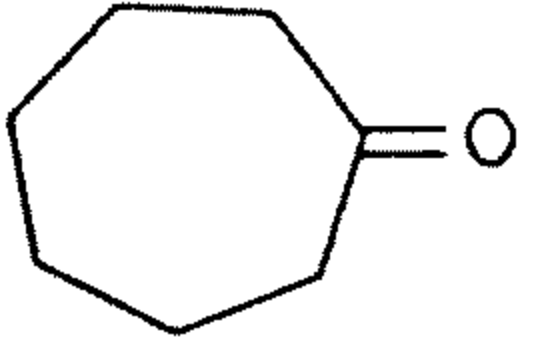
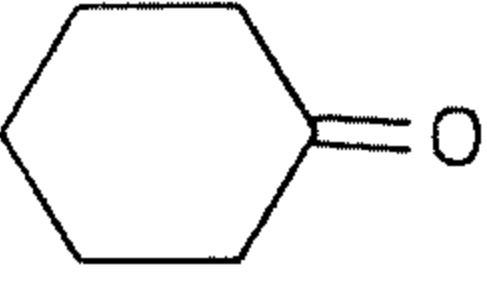
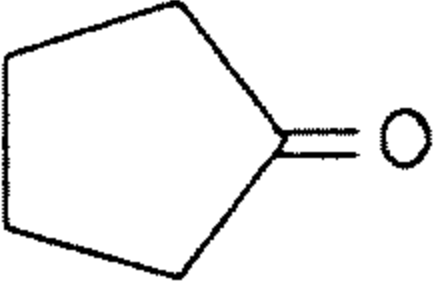
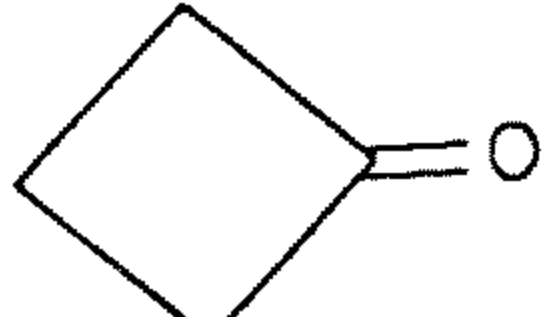
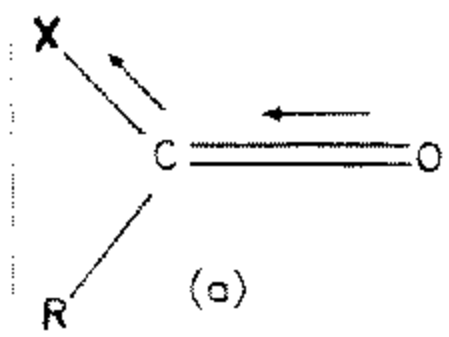
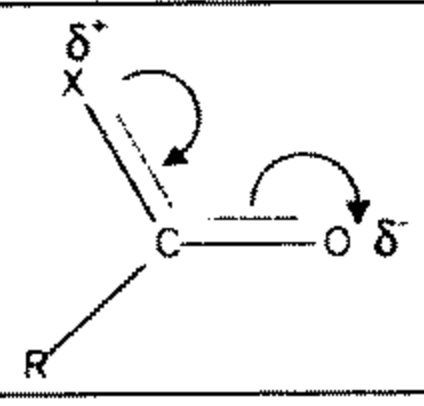
				
$\nu_{C=CH_2}$	1651 cm^{-1}	1657 cm^{-1}	1690 cm^{-1}	1750 cm^{-1}
				
$\nu_{C=O}$	1699 cm^{-1}	1710 cm^{-1}	1772 cm^{-1} 1740 cm^{-1}	1775 cm^{-1}

Table 2. The variation of $\nu_{C=O}$ frequency due to the inductive and resonance effects of X

(a) Inductive effect of X Shortens C=O bond length ↓ ↑f, ↑ $\nu_{C=O}$		
X	$\nu_{C=O}$ cm^{-1}	
Cl	1815-1785	
F (the most electro negative)	1869 (the highest)	
Br	1812	
OH (monomer)	1760	
OR'	1750-1735	
(b) Resonance effect of X Increase bond length C=O, ↓bond order ↓f, ↓frequency		
X	$\nu_{C=O}$ cm^{-1}	
-NH ₂	1695-1650	
-S-	1720-1690	

termolecular hydrogen bonds, the presence or absence of ring strain, the effect of electronic effect on bond strength, cis- vs. trans- configuration, etc. The exact IR spectrum of a compound is like the finger print of an individual. No two different compounds can have exactly the same IR absorption spectrum. Tables 1-2 and Figure 5 illustrate some of the applications mentioned above⁽³⁾.

It has been noticed that ring strain raises the stretching frequencies of an exocyclic double bond. This is illustrated by the $>C=CH_2$ series. This tendency is also true for the $>C=O$ stretching vibrations in aliphatic cyclic systems. However, this generalization, namely, "the ring strain increases as the ring size decreases," does not hold in the case of five- to seven-membered cyclic thioureas and ureas, reflecting the lack of significant ring strain in the five-, six- and seven-member rings of thioureas and ureas⁽³⁾. Table 2 shows how the different components of electronic effect can affect both the bond length, the force constant (f) and the $\nu_{C=O}$ stretching frequency.

Davies et al. have utilized FT-IR in a quantitative study of the effects of cholesterol on conformational disorder in dipalmitoylphosphatidylcholine (DPPC) bilayers.⁽⁸⁾ The method is based on the finding that the CD_2 rocking modes ($600 - 660 \text{ cm}^{-1}$) from the acyl chains of specifically deuterated phospholipids occur at frequencies depending upon the local geometry (trans or gauche) of the C-C-C skeleton surrounding a central CD_2 group. Three specifically deuterated DPPC, i.e. 4,4,4',4'-d₄-DPPC, 6,6,6',6'-d₄-DPPC and 12,12,12',12'-d₄-DPPC were synthesized and used in the determination of the effect of depth dependence.⁽⁸⁾

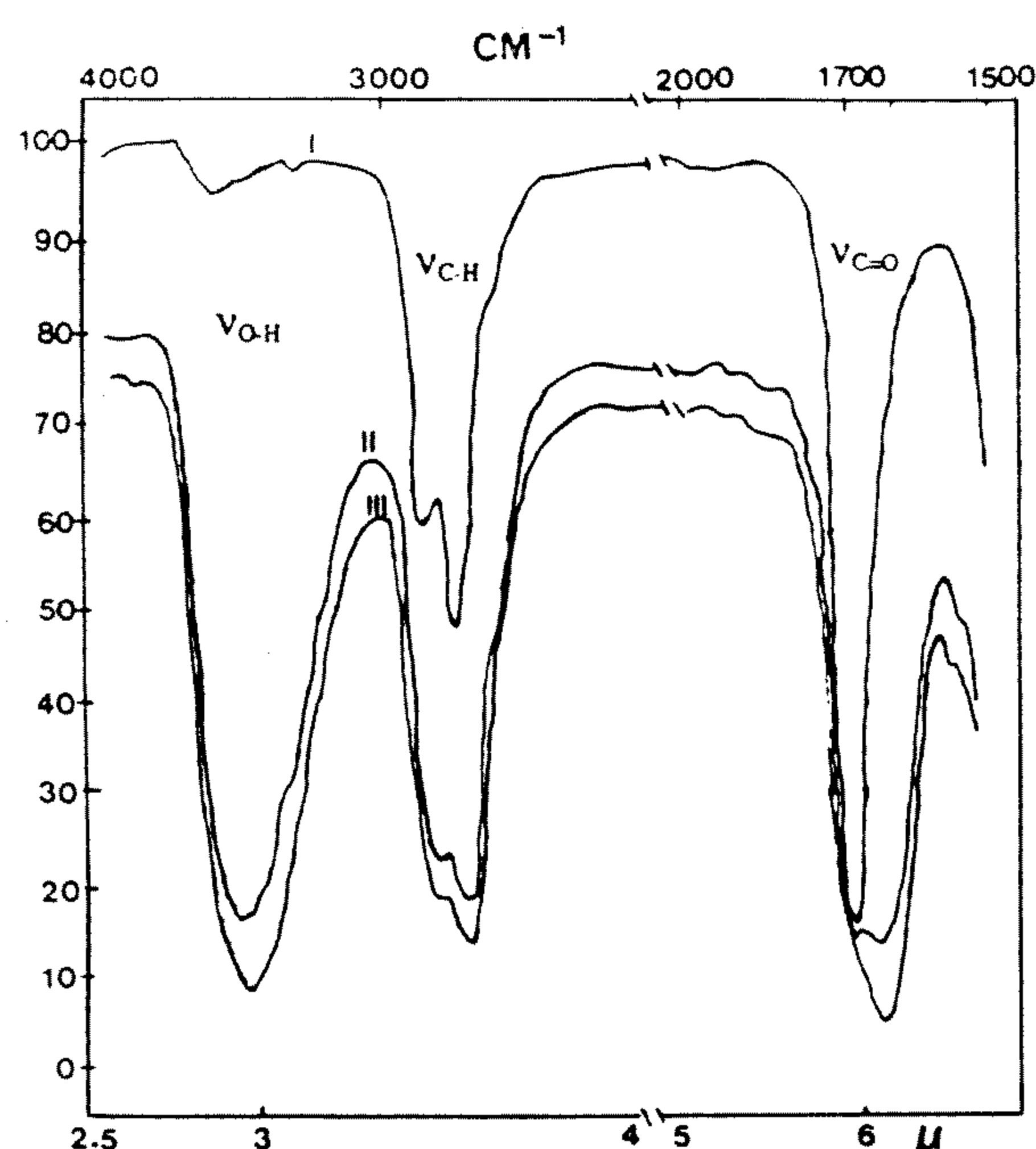


Figure 5. IR absorption spectra of N,N'-dimethylethyleneurea showing the increasing O-H band and broadening and shift of C=O band after exposure to the air, reflecting the absorption of moisture (H₂O) by the very hygroscopic nature of the compound. (adapted from ref. 3).

- I. Minimum exposure to the air.
- II. Exposed to the air for 15 minutes.
- III. Exposed to the air for 30 minutes.

Haris et al⁽⁹⁾ have employed FT-IR together with ¹³C and ¹⁵N labeling in studying protein-protein interactions. The proteins used are bacterial HPr and IIA^{mtl} of *E. Coli* phosphoenolpyruvate-dependent phosphotransferase system. It was shown in this study that in an interaction of 1:1 molar ratio of these two proteins, the overlap of absorbance of the amide I band ($\nu_{C=O}$, see Table 3) arising from the peptide group of the unlabeled proteins made it impossible to determine the contribution from each protein to the absorbance. It was further shown that uniform ¹³C-labeling of HPr shifted the amide I band of this protein by 38 — 45 cm⁻¹ toward lower frequency and revealed the previously overlapped amide I band of the unlabeled IIA^{mtl} (1643 cm⁻¹). This application of ¹³C labeling demonstrates the potential of studying protein-protein interactions using FT-IR. With proper selection of systems and labeling, this type of study can be extended to enzyme-substrate and protein-ligand interactions as well as β -sheet protein/ α -helix protein interactions.⁽⁹⁾

FOURIER TRANSFORMATION IN NMR AND IR

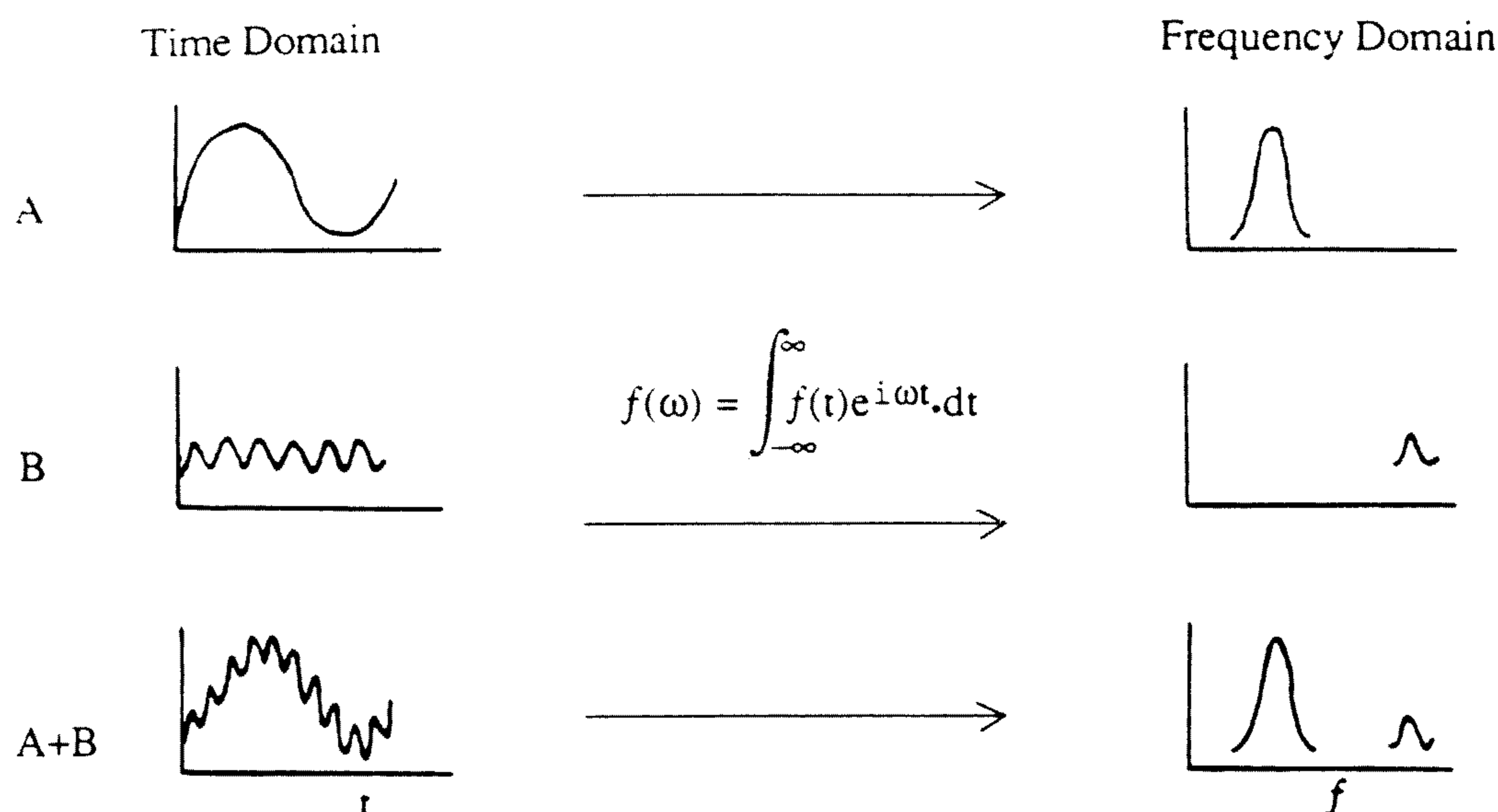


Table 3. FT-IR spectra of unlabeled and ^{13}C and ^{15}N labeled HPr protein and interaction with IIA^{mtl} protein.

	Frequency in cm^{-1}		
	Amide I $\nu_{\text{C=O}}$	Amide II $\delta_{\text{N-H}}$	Carboxylate ν_{COO^-}
Unlabeled HPr in $^2\text{H}_2\text{O}$ at 20°C	1636(s) — — — — — 1652(shoulder) 1682(shoulder)	1530-1550 (weak, due to) ^1H - ^2H exchange)	1565(m) — — — — —
Unlabeled IIA^{mtl}	1645(s) (-38)		1563(m) (-41)
^{15}N -labeled HPr	1634(s) 1650(shoulder) 1680(shoulder)	1450 (overlaps with $\text{H-O-}^2\text{H}$ absorbance)	1567(m)
$^{13}\text{C}/^{15}\text{N}$ -labeled HPr in $^2\text{H}_2\text{O}$ at 20°C	1598(s) ← (-51)	"	1524(m) ←
1:1 M ratio of $^{13}\text{C}/^{15}\text{N}$ -labeled HPr + unlabeled IIA^{mtl}	1643(s) 1585(s) ← (clearly separated)	"	1524 1563(m)

To resolve complex spectrum due to overlap of different absorption peaks, a complex mathematical digital computer program (fast Fourier transform) is usually used in modern equipment to convert the complex amplitude waveforms in the time domain to separable amplitude waveforms in the frequency domain. This is shown in the following radiofrequency (RF) electromagnetic waves in the NMR signal (10,11), this increases the sensitivity by a factor of ten and cuts down the sweep time required. The same principle is also applicable in IR and far-IR spectroscopy.

FUNDAMENTAL EQUATIONS INVOLVED IN NMR SPECTROSCOPY AND APPLICATIONS

Energy : $E=h\nu$ (planck's constant \times frequency)

$$\nu = \frac{\gamma H_0}{2\pi} \quad (4)$$

or $\gamma \cdot H_0 = 2\pi \cdot \nu$(4) The fundamental NMR equation

γ = Magnetogyric ratio (a fundamental nuclear constant, see Table 4)

H_0 = Magnetic field strength

γ is further related to the magnetic moment μ (see Table 4).

$$\text{by } \gamma = \frac{2\pi\mu}{hI} \quad (5)$$

I = Nuclear spin number ($I=1/2$ for ^1H)

If we introduce a proper frequency ν , it will be in resonance with ω_0 the precessional frequency, ΔE can be absorbed to flip the nucleus from low to high energy state.

$$\Delta E = h \cdot \nu = h(\gamma \cdot H_0 / 2\pi) \text{ by substituting eq. (5) for } \gamma$$

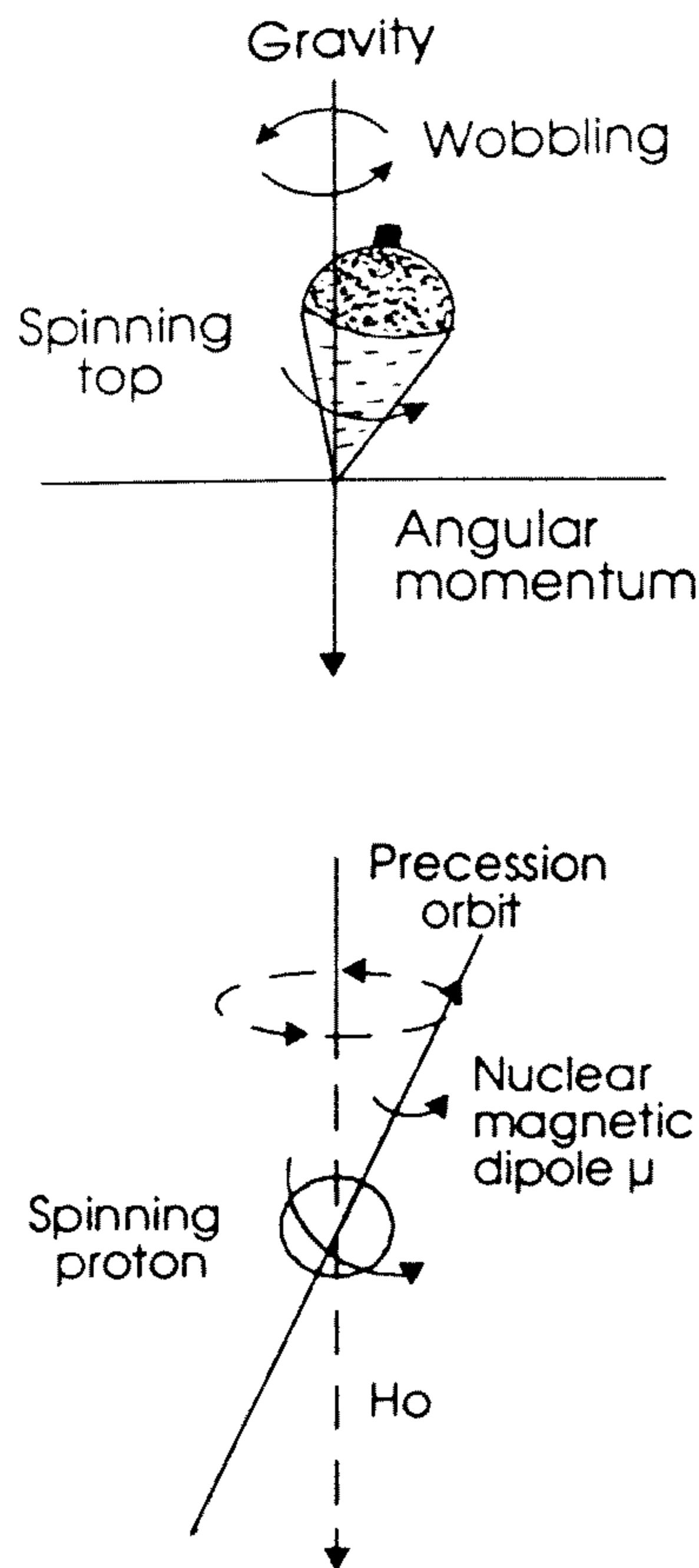
The precessional angular velocity ω_o is proportional to H_o

$\omega_o = \gamma \cdot H_o$ (6)

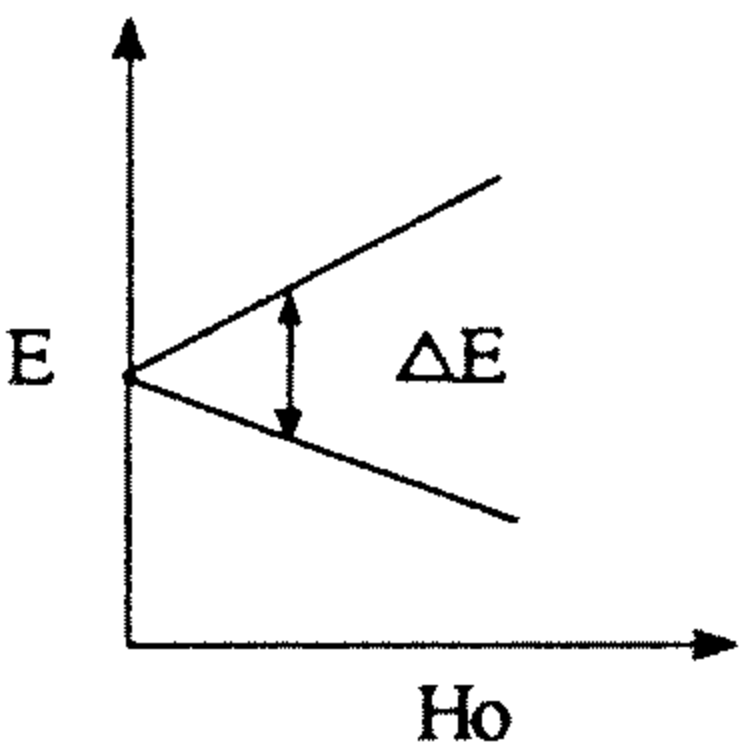
By combining eq. (4) and (6) we have:

$\gamma \cdot H_o = 2\pi \cdot \nu$ (7)

$\omega_o = 2\pi \cdot \nu$ (8)



we have : $\Delta E = h \cdot \nu = \mu \cdot H_o / I$ (9)



Several nuclei of biomedical interest (see Table 4) have a spin number I of 1/2 and a uniform spherical charge distribution, while deuterium (²H) has an I of 1. The number of orientations of these nuclei (with I of 1/2) may assume in an external uniform magnetic field is equal to 2I+1=2. Among these nuclei, ¹H, ¹³C, ¹⁵N, ¹⁹F and ³¹P are commonly employed in biomedical and pharmaceutical research. Because of the low natural abundance of ¹⁵N specially designed instrument like a Bruker WH-180 spectrometer operating at 18.25 MHz in the FT mode and large (25 mm) sample tubes are required to produce interpretable spectrum.⁽¹²⁾(see Figure 6 for details).

Because of the 100% natural abundance both ¹⁹F and ³¹P containing compounds are gaining popularity in biomedical and pharmaceutical research. For example, El-Tahtawy and Wolf⁽¹³⁾ of USC have used ¹⁹F-NMR in studying the intratumoral metabolism, modulation and pharmacokinetics of 5-fluorouracil *in vivo* in mice. Fariño et al.⁽¹⁴⁾ of National Eye Institute have used ¹⁹F NMR in the quantitation of lens aldose reductase activity (implicated in diabetic compli-

Table 4. Properties of several nuclei of biomedical interest

Isotope	Natural abundance	Relative sensitivity at constant field	Magnetic moment μ	Spin number	Magnetogyric ratio (γ_N) (radian sec ⁻¹ gauss ⁻¹)
¹ H	99.9844	1.00	2.79268	1/2	26,753
² H(² D)	1.56 × 10 ⁻²	9.64 × 10 ⁻²	0.85739	1	4,107
¹³ C	1.108	1.59 × 10 ⁻²	0.70220	1/2	6,728
¹⁵ N	0.365	1.04 × 10 ⁻³	-0.28304	1/2	-2,712
¹⁹ F	100	0.834	2.6273	1/2	25,179
³¹ P	100	6.64 × 10 ⁻²	1.1305	1/2	10,840

Adapted from ref. 2.

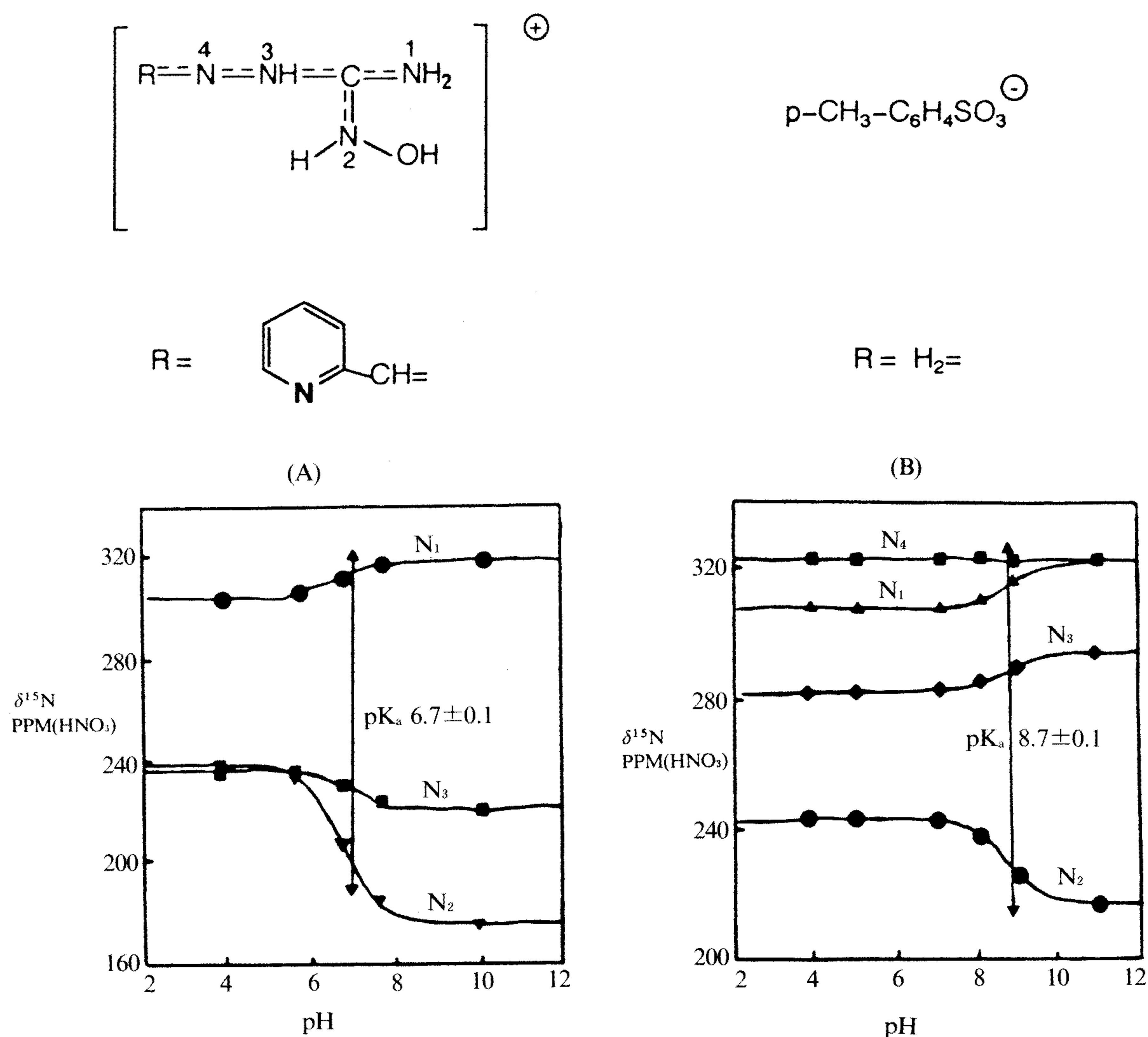


Figure 6. (A). ^{15}N NMR chemical shift changes with pH of 2-[(2-pyridylmethylene) diazanyl]-N-hydroxymethanaminidinium 4-methylbenzenesulfonate in water solution; (B). ^{15}N NMR chemical shift changes with pH of 1-amino-3-hydroxy-guanidine 4-methylbenzenesulfonate. These spectra were taken at the natural-abundance level in 25-mm sample tubes, with broad-band decoupling, a repetition rate of 5 s, and a pulse width of 35 μs (34° flip angle). The concentrations were about 0.3 M. The ^{15}N NMR chemical shifts are reported in parts per million upfield from an external standard made up to be 1M H^{15}NO_3 in D_2O (adapted from ref. 12).

cations like cataract, keratopathy, retinopathy, and neuropathy) using 3-deoxy-3-F-D-glucose as the substrate. Martin and his coworkers⁽¹⁵⁾ of the Pennsylvania State University have employed ^{31}P -NMR to evaluate postischemia renal ATP and pH levels after ATP- MgCl_2 treatments in rabbits⁽¹³⁾. It was found that ATP- MgCl_2 treatment improves postischemic functional parameters without functioning as a direct source

of ATP or its precursors. The data support the emerging concept that intracellular acidosis protects cells from reperfusion injury.⁽¹⁵⁾

SOLID-STATE NMR AND 2D NMR SPECTROMETRY

I. Solid-State NMR and its application in pharmaceutical Sciences

NMR has been used in pharmaceutical sciences in the elucidation of structures of compounds, investigation of chirality of drug molecules, determination of cellular metabolism, and the study of biological macromolecules such as proteins, nucleic acids, and polysaccharides. In most of these cases, solution phase NMR has been applied. Since, many pharmaceutical products are in solid forms, solid phase NMR may be more convenient and useful in the direct analysis of pharmaceutical products.

Comparison to solution-phase, molecules in solid-phase can not move freely. Due to dipolar interactions which do not average out to zero, and chemical shift anisotropy (CSA), solid-phase NMR spectra will be broad, featureless if conventional solution-phase NMR acquisition techniques are used. High-power proton decoupling, magic-angle spinning (MAS), and cross-polarization have to be used in the acquisition process of solidphase NMR (see Figure 7)⁽¹⁶⁾.

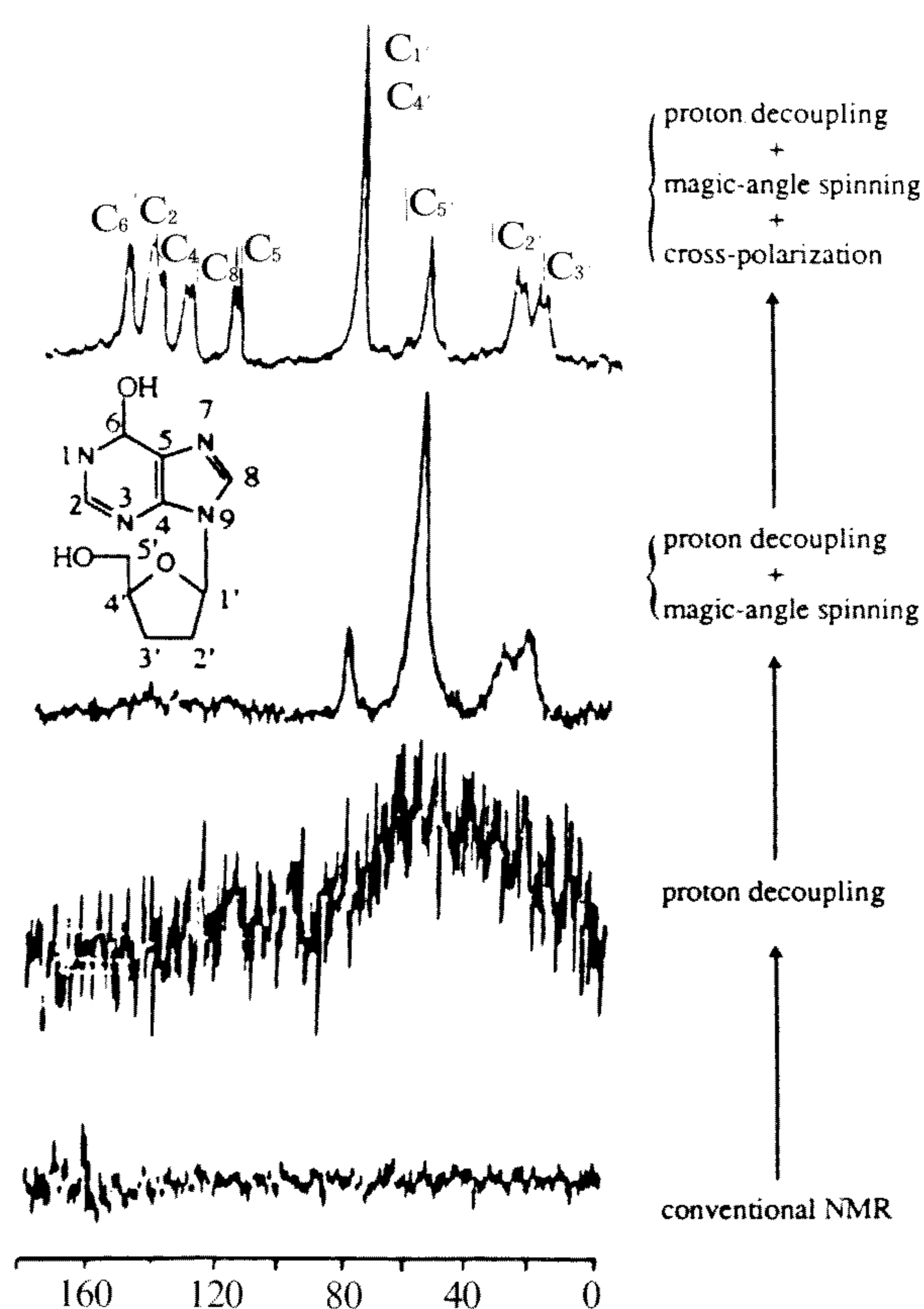


Figure 7. Solid-state ^{13}C spectra of didanosine (adapted from ref. 16)

Dipolar interactions can be solved through simple high-power proton decoupling fields which is similar to solution-phase NMR techniques. Cross-polarization is the technique in which the magnetization of the rare spin system like ^{13}C can be enhanced by the transfer of magnetization from the abundant spin system like proton. This technique has been used in a number of 2D NMR techniques.

Molecules in the solid state are in fixed orientations with respect to the magnetic field. This produces chemical shift anisotropic (CSA) effects. In solution-phase NMR, a spectrum yields "average" chemical shift values which are characteristic of the magnetic environment for a particular nucleus. The average signal is due to the isotropic motion of the molecules in solution. For solid-phase NMR, the chemical shift value is also characteristic of the magnetic environment of a nucleus, but a specific functional group oriented perpendicular to the external magnetic field (B_0) will give a sharp signal characteristic of the particular orientation. A specific group orientated parallel to B_0 will also produce a sharp signal. In solid state, a random distribution of all orientations of the molecule exists. This random distribution will give a very broad NMR signal (see Figure 8). It has been known that spinning could remove broadening caused

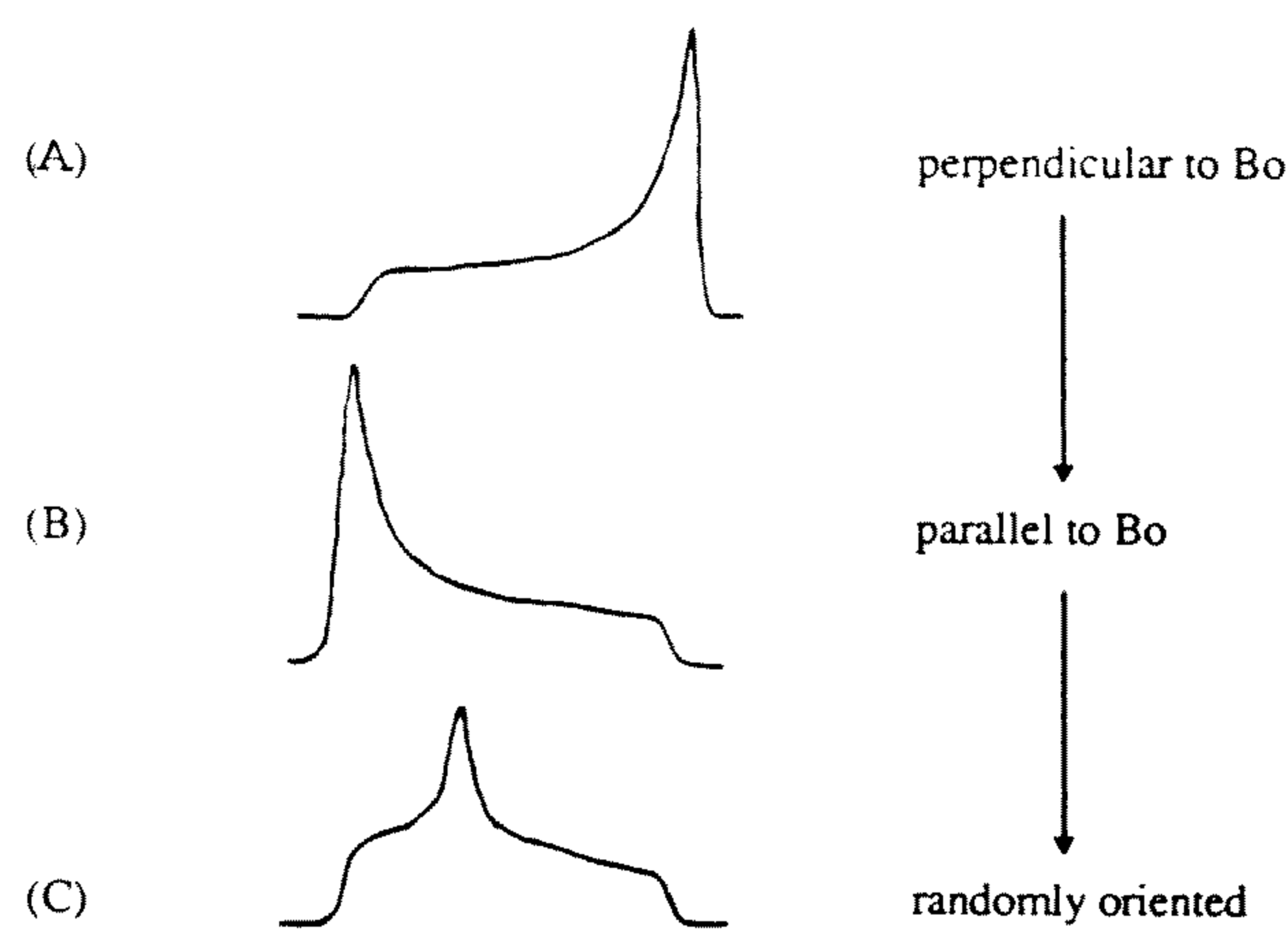


Figure 8. Schematic representation of ^{13}C signal with different orientations of functional group (adapted from ref. 16)

by CSA⁽¹⁶⁾. The concept of magic-angle spinning (MAS) arises from the understanding of the shielding constant, σ .

$$\sigma_{zz} = \sum \sigma_i \cos^2 \theta_i$$

This constant is a tensor quantity, and can be related to three principal axes where σ_i is the shielding at the nucleus when B_0 aligns along the i th principal axis, and θ_i is the angle this axis makes with B_0 . Under mechanical spinning, this relationship becomes time dependent and a $(3\cos^2\theta_i - 1)$ term arises. By spinning the sample at the so-called "magic angle" of 54.7° ; this term becomes zero and thus remove the spectra broadening due to CSA. The spinning rate is also important in order to minimize side bands (see Figure 9)⁽¹⁷⁾. Solid-state NMR has been successfully used in the study of polymorphism or pseudopolymorphism⁽¹⁸⁾ and in the quantitative analysis of anhydrous carbamazepine and carbamazepine dihydrate⁽¹⁹⁾.

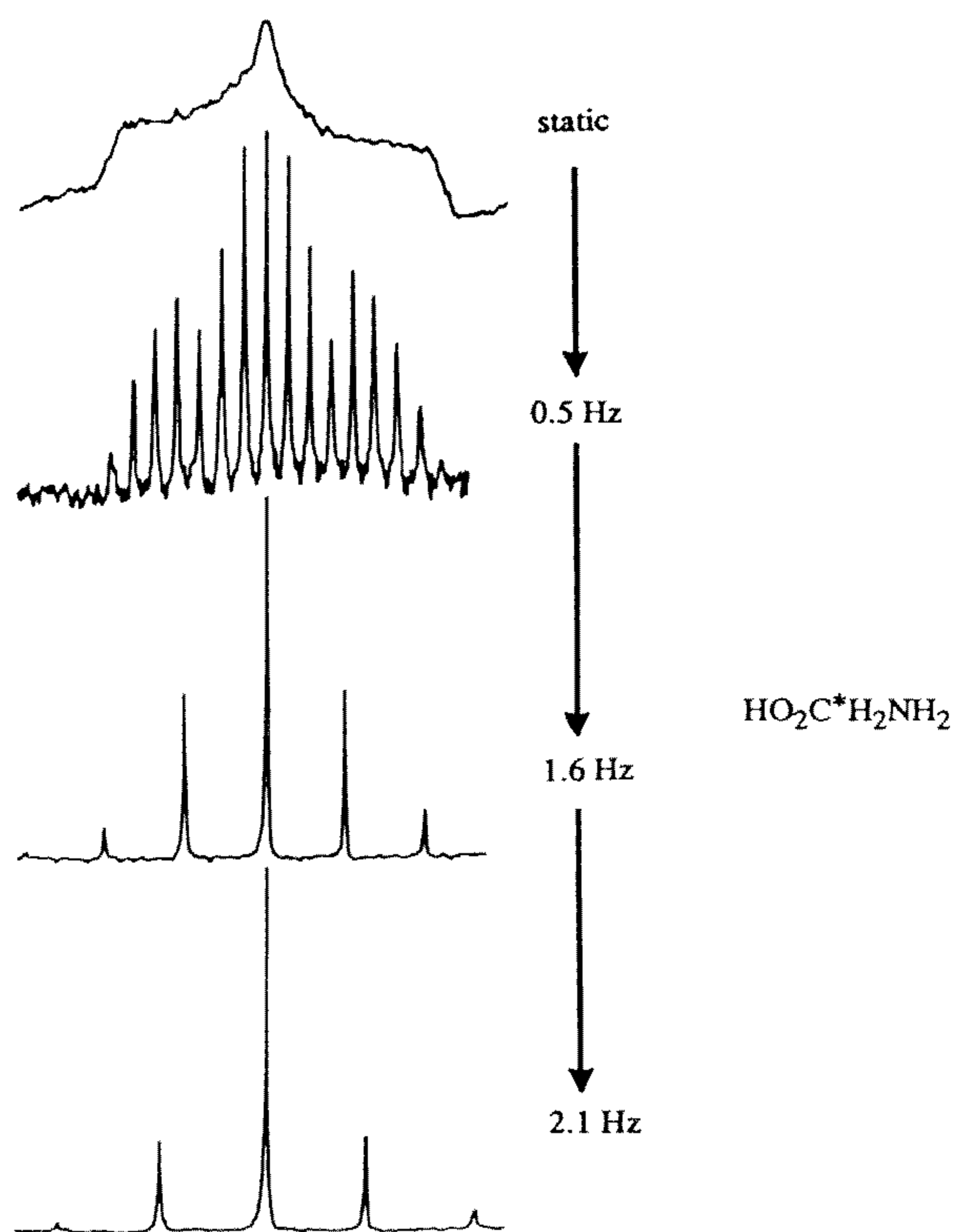


Figure 9. Solid-state ^{13}C NMR of the carboxyl carbon of glycine with different magic-angle spinning rate (adapted from ref. 19).

II. 2D NMR spectra

The most important development in modern NMR is the expansion of NMR into two frequency dimensions. Two-dimensional (2D) NMR methods and related one-dimensional (1D) multipulse sequences have given chemists enormous power in the structural analysis of a broad range of compounds. Nowadays, chemists can solve the structural problem of many organic compounds, peptides, even polysaccharides with very complicated structures⁽²⁰⁻²²⁾ by just using combination of various spectra of both 1D and 2D NMR. Various techniques are briefly discussed as follows, for more detailed explanations of the procedures and requirements, the original references should be consulted:

(I). Homonuclear Correlation Spectroscopy (COSY) and Double-Quantum filtered COSY (DQFCOSY)

COSY is a technique used most frequently in 2D-FT NMR. In normal COSY, both vertical and horizontal axes provide for ^1H chemical shift. In COSY, ^1H - ^1H connectivities can be obtained through the examination of cross peaks which are the results of spin-spin couplings of protons. Figure 10 and 11 are the 1D ^1H -NMR and 2D COSY of geraniol, respectively. In COSY spectrum, the cross peaks between C-6 and C-5, C-2 and C-9 protons are clearly shown. Recently, Wang and Lee have successfully identified the isomerization products of cefuroxime by using ^1H - ^1H COSY 2D NMR (Figure. 12)⁽²³⁾, where the coupling of C2-H and C-4-H is clearly shown in the isomerized product, but not in the starting material which does not have C4 proton.

In the COSY, singlet peaks are often too intense so that S/N (signal to noise ratio) of the overall spectrum may be poor. This often results in considerable overlap along the diagonal, and thus it is difficult to make assignments. This can be alleviated by multiple quantum filtration. Double-quantum filtration (DQFCOSY) is one of the commonly used methods. Figure 13 is the

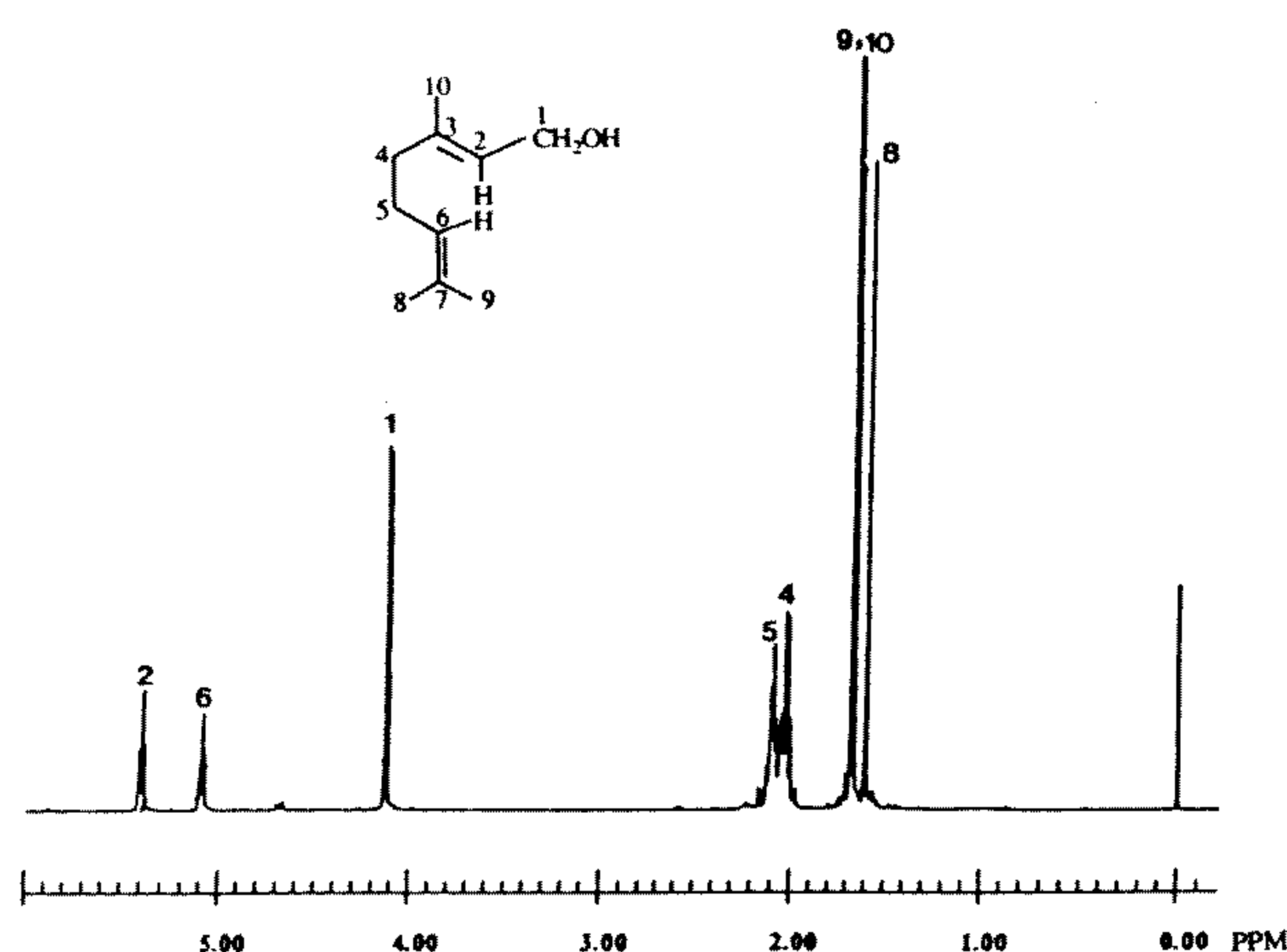


Figure 10. The ^1H spectrum of geraniol in CDCl_3 at 500 MHz (adapted from ref. 2, p. 271).

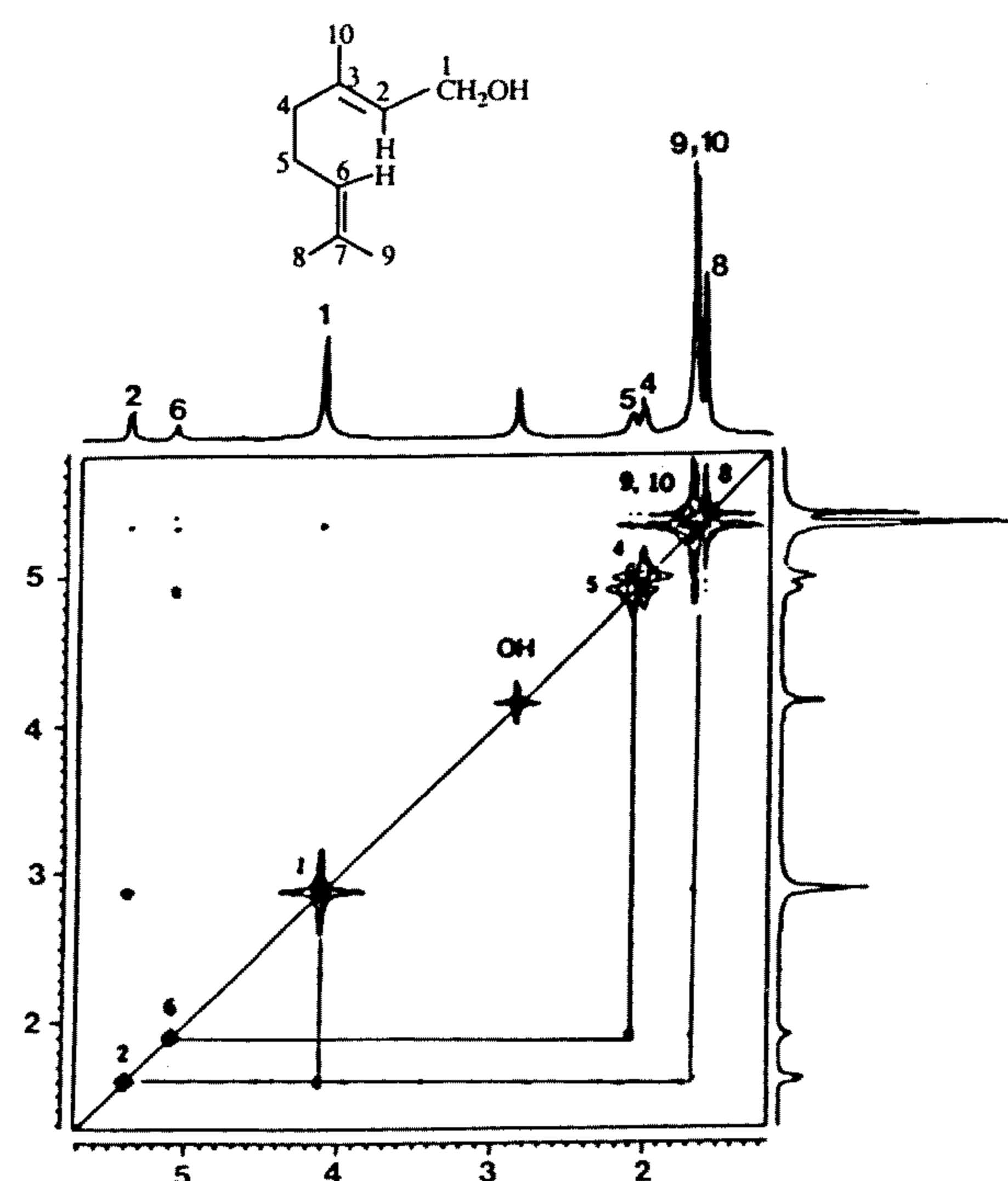


Figure 11. The COSY spectrum of geraniol in CDCl_3 at 500 MHz (adapted from ref. 2, p. 274). Note the cross peaks between C-6 and C-5, C-2 and C-9 protons.

DQFCOSY spectrum of geraniol. The peaks of C-8,9 and 10 methyl group protons on the diagonal line are much more clearly separated than in basic COSY spectrum (Figure. 11), and the cross peaks between C-6 and C-8, C-9 protons are also clearly interpretable in Figure 13.

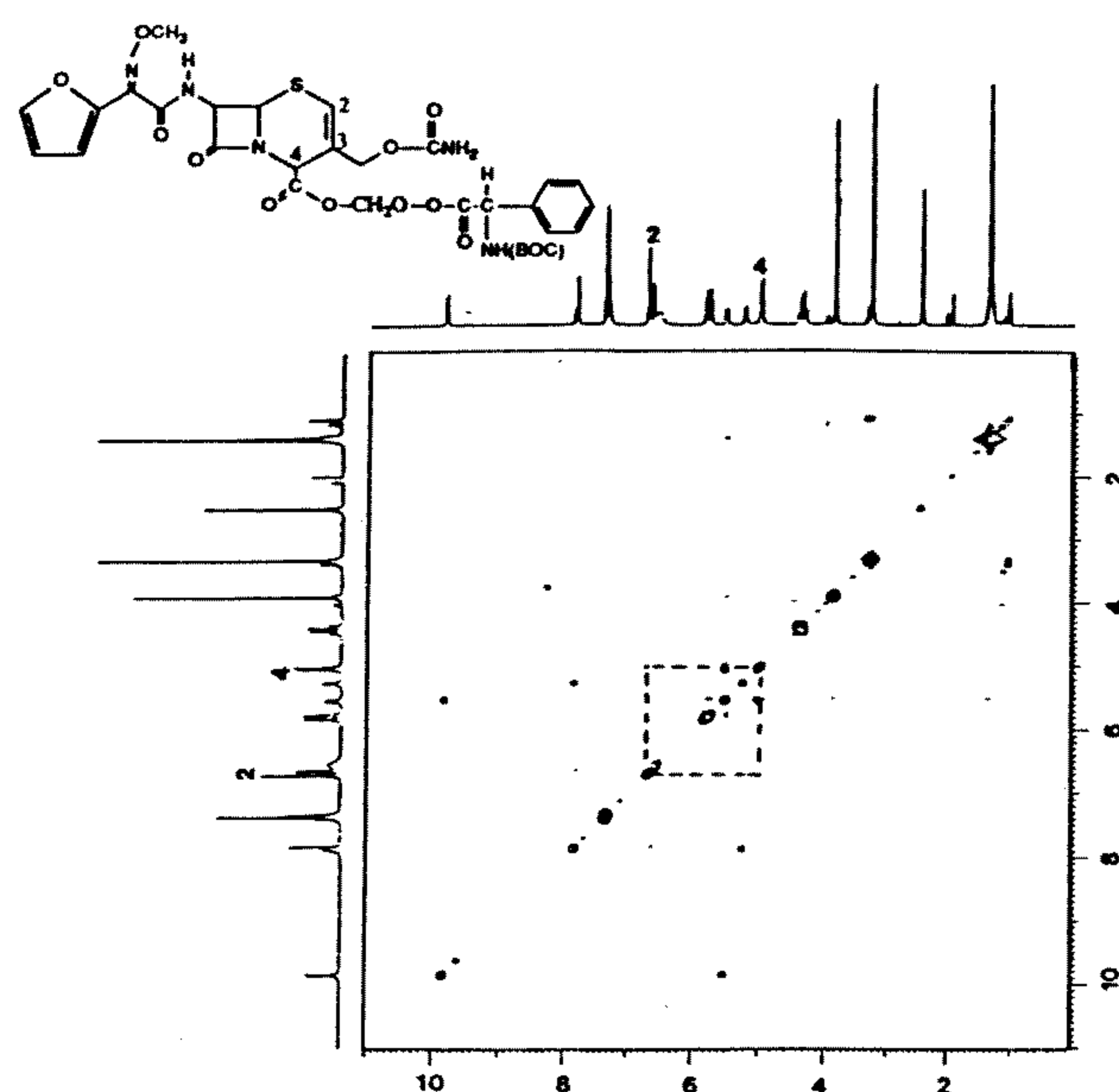


Figure 12. The COSY spectrum of compound 1b in DMSO-d_6 at 300 MHz (adapted from ref. 23). Note the coupling of C2-H and C4-H.

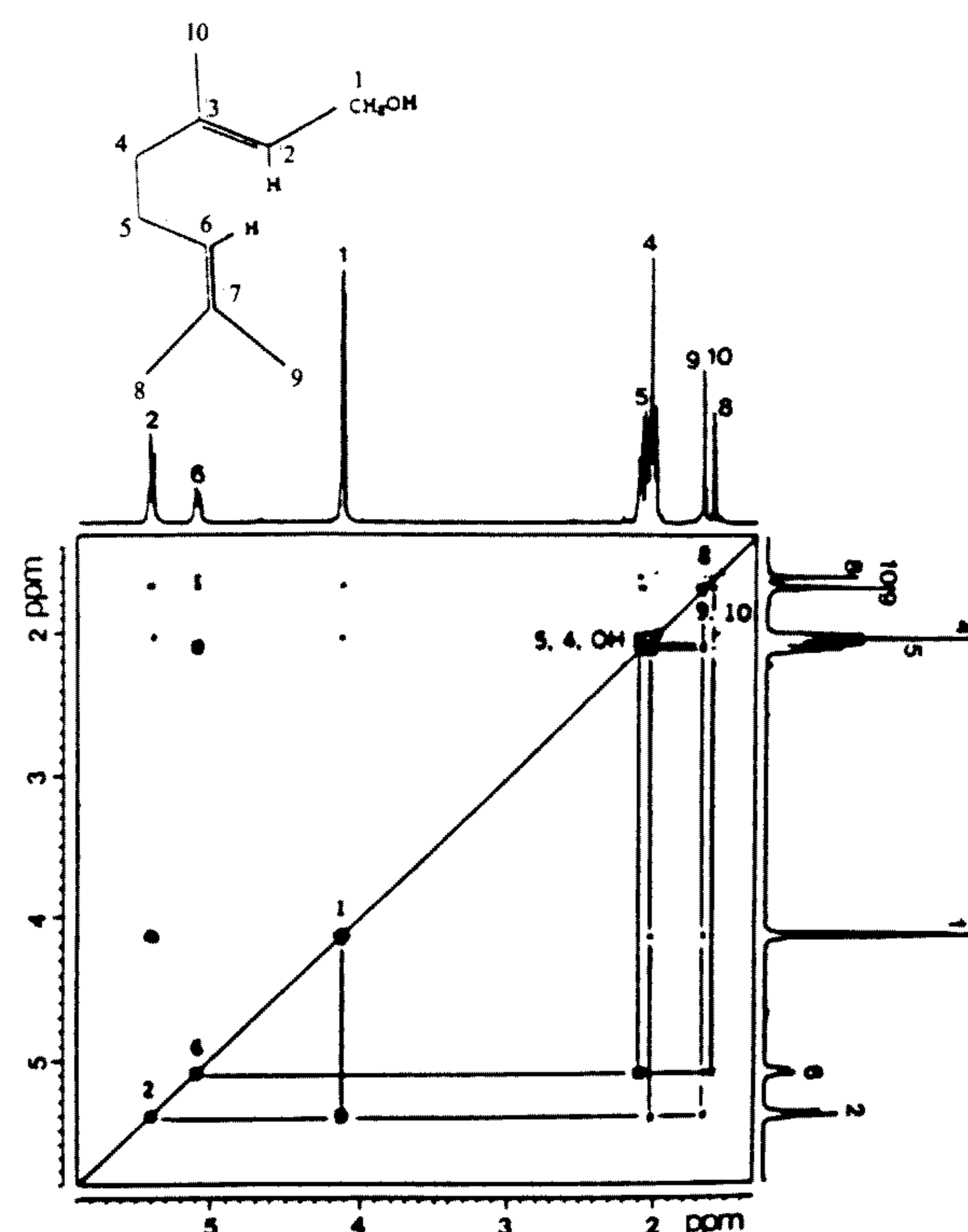


Figure 13. The DQF-COSY spectrum of geraniol in CDCl_3 at 500 MHz (adapted from ref. 2, p.275). Note that the peaks of C-8,9 and 10 methyl group protons on the diagonal line are much more clearly separated than in COSY spectrum (Figure 11).

(II). *Nuclear Overhauser and Exchange Spectroscopy (NOESY)*

In NOESY spectrum, the interactions among spatially close protons can be seen as cross peaks. Therefore, NOESY spectrum is very sensitive to the inter-proton distance. This is useful in determining the spatial conformations of molecules. Figure 14 shows the NOESY spectrum of β -ionone. Because the side chain of β -ionone does not have a fixed conformation, the 1,1'-Me has cross peaks with both C-7 and C-8 protons.

(III). *^1H - ^{13}C single bond multiple-quantum correlation spectrum (HMQC)*

In HMQC spectrum, all the cross peaks from the carbon atoms to respective protons attached will be seen. Therefore, it is very useful in assigning the ^1H - ^{13}C connectivities. Figure 15 shows the HMQC spectrum of strychnine. All the cross peaks between the proton(s) and the carbon atoms to which they are attached are presented.

(IV). *^1H -detected ^1H - ^{13}C Multiple-Bond Correlation spectrum (HMBC)*

Long-range H-C interactions of two and three intervening bonds ($^2J_{\text{CH}}$ and $^3J_{\text{CH}}$) of compound can be seen as cross peaks. This is useful in determination of the skeleton of a given compound. In Figure 16, a number of long-range H-C coupling can be seen, especially 14-C to 20-H ($^3J_{\text{CH}}$) and 8-H ($^3J_{\text{CH}}$)

(V). *2D Incredible Natural Abundance Double Quantum Transfer Experiment spectroscopy (2D-INADQUATE)*

2D-INADQUATE is the method used to analyze adjacent (coupled) ^{13}C - ^{13}C pairs from the correlation of double quantum transition frequency and chemical shifts. It is very useful in the determination of the connectivity of carbon atoms, in other words, in the establishment of the carbon skeleton. The 2D-INADQUATE spectrum of L-menthol is shown in Figure 17. From this spectrum, one can connect all carbon atoms from left to right.

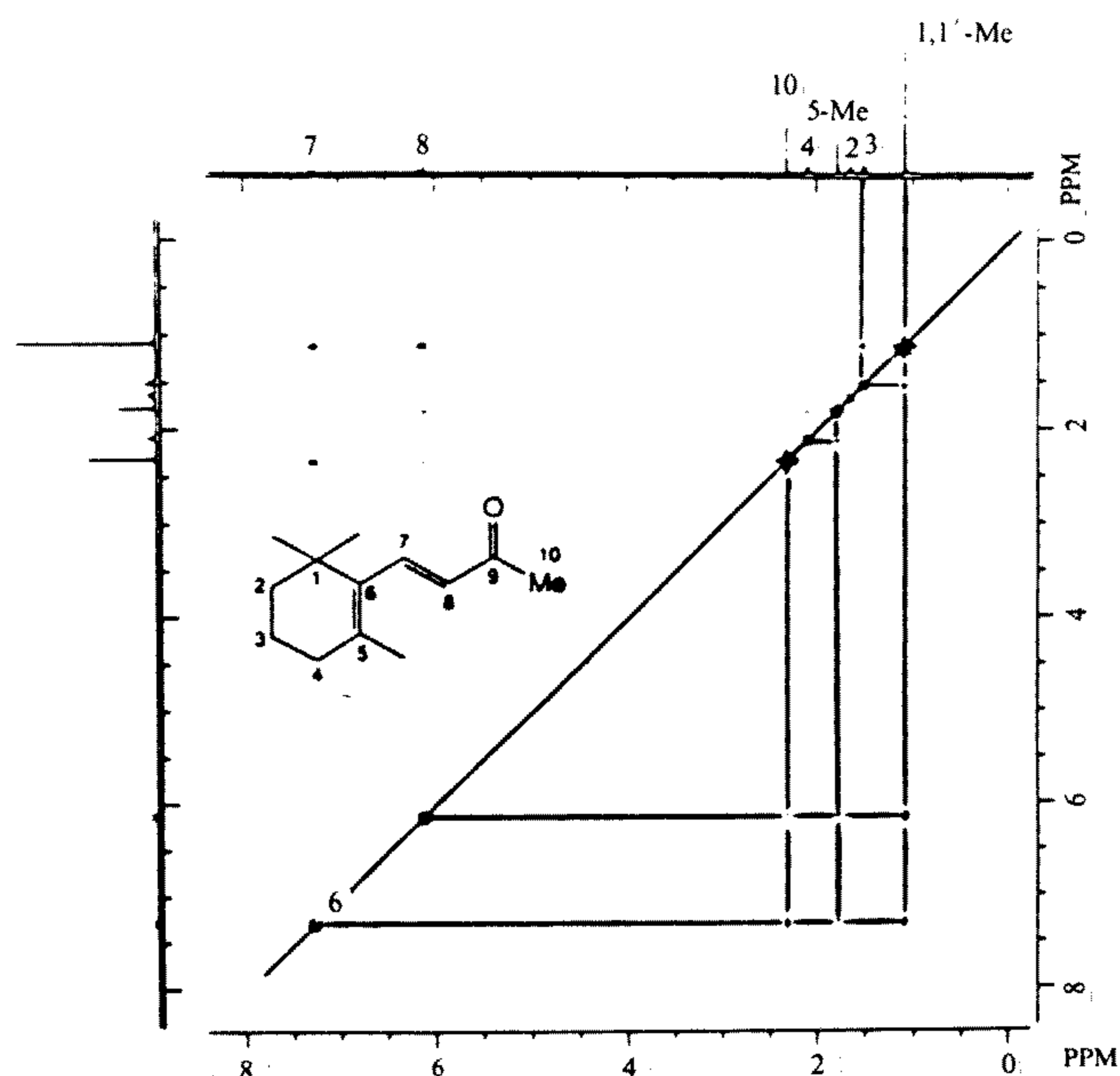


Figure 14. The NOESY spectrum of β -ionone in CDCl_3 at 360 MHz (adapted from ref. 23, pp.118). Note the cross peaks between the 1,1'-Me protons with both C-7 and C-8 protons.

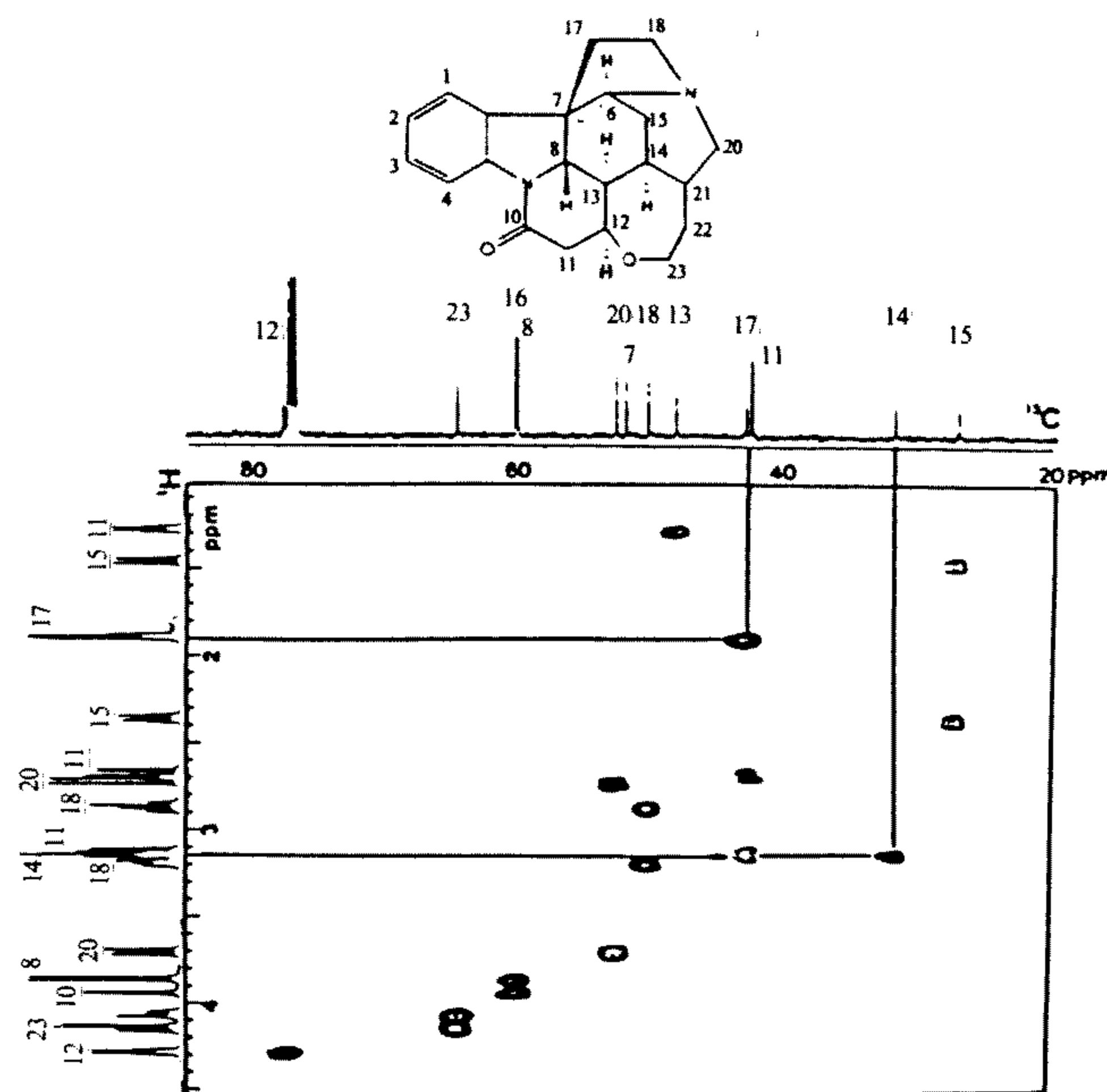


Figure 15. The HMQC spectrum of strychnine in CDCl_3 at 500 MHz (adapted from ref. 23, pp.160). A window of 1-4.5 PPM chemical shift is selected for ^1H , and 20-80 PPM is selected for ^{13}C . This spectrum shows all the couplings of ^{13}C s and the protons directly attached to them.

A summary of 2D NMR techniques and their uses is presented in Table 5.

Table 5. Summary of 2D NMR spectra

2D Spectrum	Information	Uses
COSY and DQFCOSY	proton-proton interactions	establishment of ^1H - ^1H connectivity
NOESY	interactions among spatially close protons	analysis of spatial distance and conformations
HMQC	interactions between carbon and respective protons attached.	^1H - ^{13}C connectivity
HMBC	long-range proton-carbon interactions	establishment of skeleton and conformation
2D-INADQUATE	adjacent ^{13}C - ^{13}C interactions	establishment of carbon skeleton

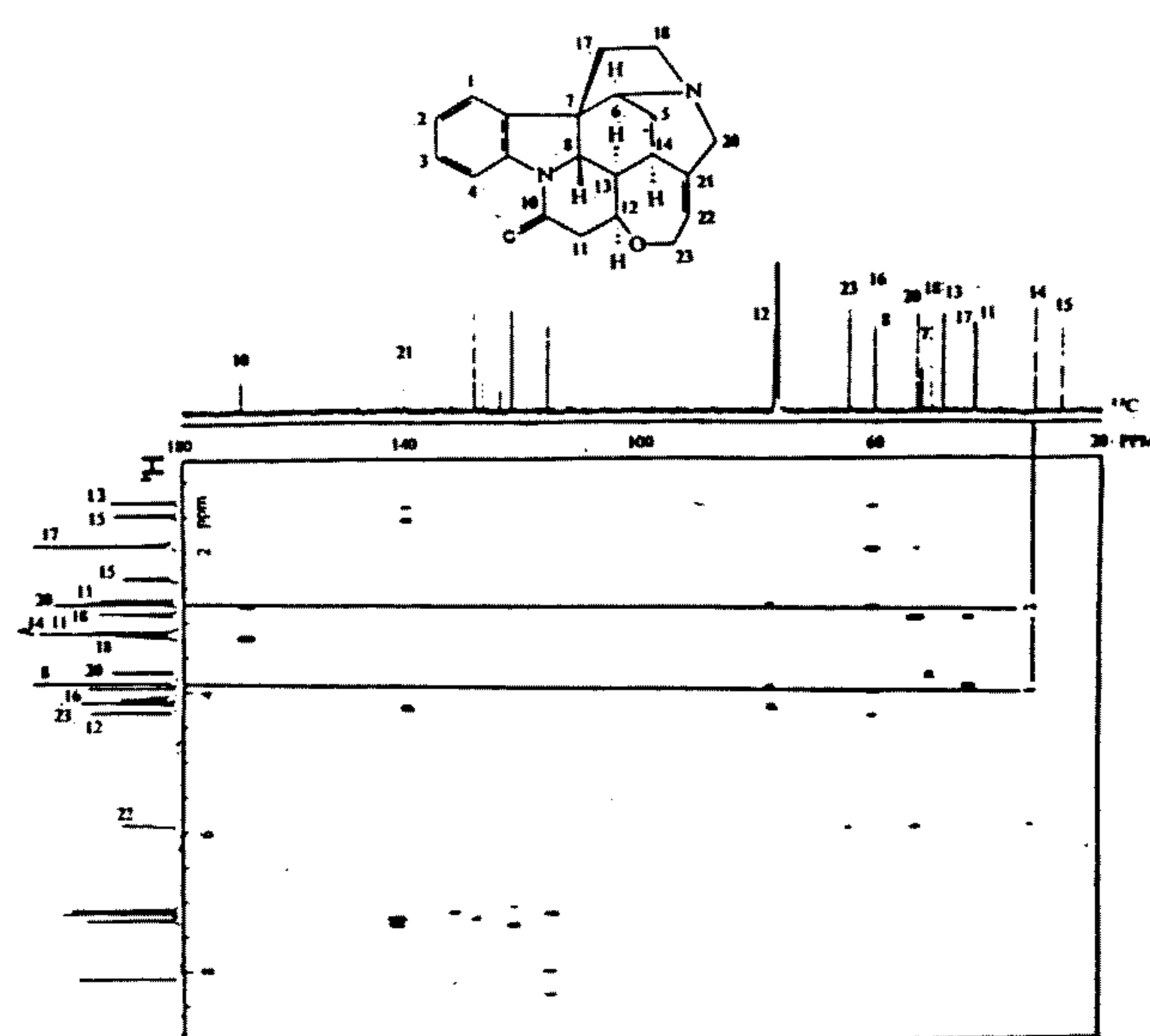


Figure 16. The HMBC spectrum of strychnine in CDCl_3 at 500 MHz (adapted from ref. 23, pp.168). A window of 1-9 PPM chemical shift is selected for ^1H , and 20-180 PPM is selected for ^{13}C . This spectrum shows long range couplings between ^{13}C and ^1H , e.g. ^{13}C -14 with C-20 and C-8 protons.

CONCLUDING REMARKS

Both 2D and 3D NMR methods have been used in studying protein structures, protein-protein interactions, complex carbohydrates, nucleic acids, and DNA/RNA and ligand interactions (25). In addition, spectroscopic methods offer many possibilities of *in vivo* (e.g. Magnetic resonance imaging, ^{19}F -FMR drug monitoring)

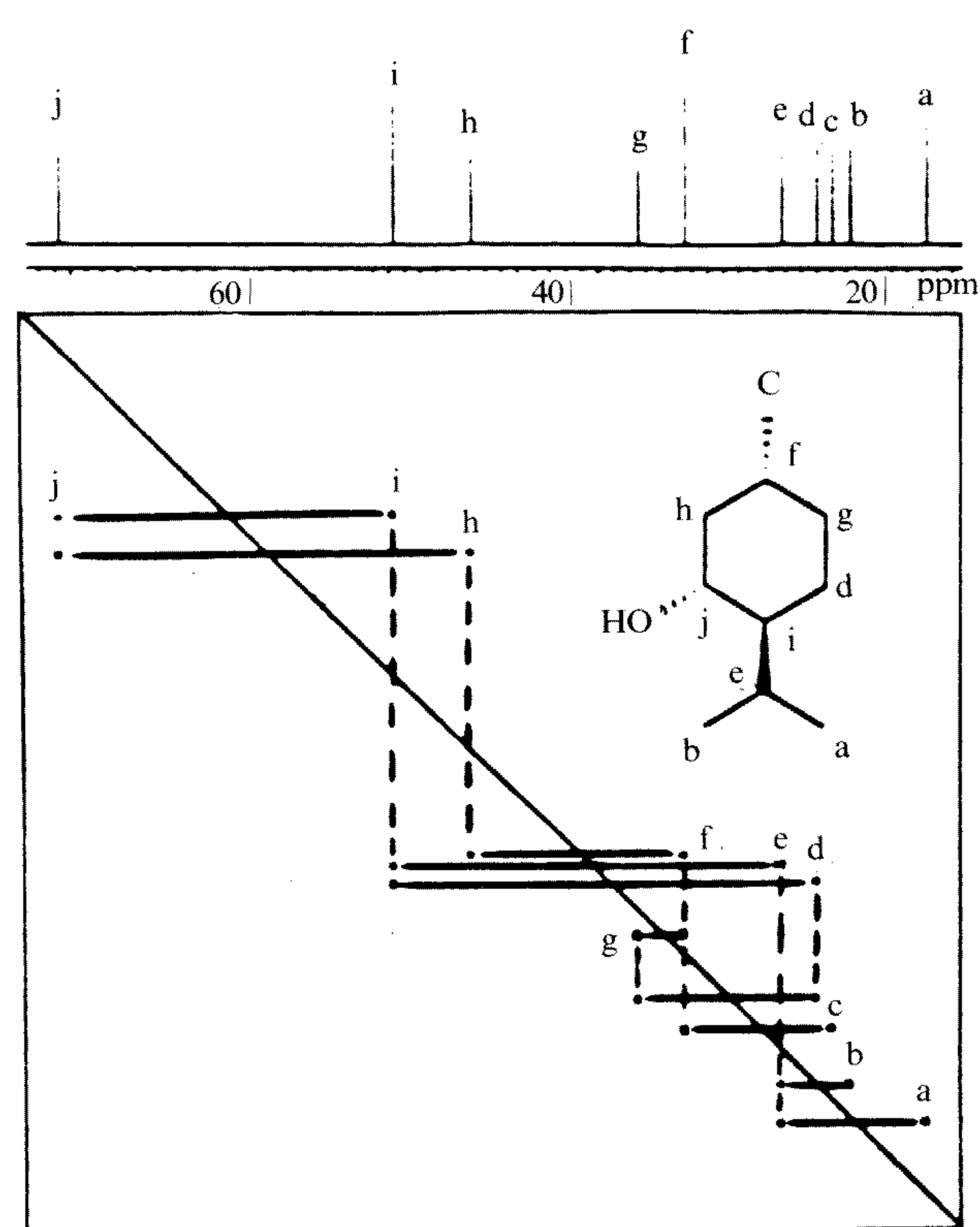


Figure 17. The 2D-INADQUATE spectrum of L-menthol in C_6D_6 at 100 MHz (adapted from ref. 23, pp. 178). The carbon skeleton of the compound is clearly established by the pattern of connection (e.g. a to e, e to b and i, etc).

non-invasive, nondestructive quantitative as well qualitative means of analysis of drugs and biochemical substances of interest. With proper experimental design and instrumentation these me-

thods may provide real-time information which can not be achieved by other analytical methods. It is expected that even more applications of the methods reviewed will appear in the literature in the near future.

REFERENCES

1. Bauman, R.P. 1962. Absorption Spectroscopy. pp. 1-25. John Wiley & Sons, Inc. New York, NY.
2. Silverstein, R.M., Bassler, G.C. and Morrill, T.C. 1991. Spectrometric Identification of Organic Compounds, Wiley & Sons, Inc. 5th ed. pp. 1-419.
3. Lien, E.J. 1966. Dipole Moment, Structure And Activity Of Cyclic Ureas, Thioureas And Related Compounds. Ph.D. dissertation, pp.1-112. University of California San Francisco, San Francisco, California.
4. Lee, A.R. 1992. Derivative spectroscopy and its applications in drug analysis. Chin. Pharm. J. 44 : 87-96.
5. Metwally, M.F. 1992. First derivative spectrophotometric determination of propranolol in the presence of its degradation products. Chin. Pharm. J. 44 : 407-412.
6. El-Maamli, M. 1992. First derivative spectrophotometric determination of fluorometholone and neomycin sulphate in combination. Chin. Pharm. J. 44 : 451-455.
7. Cavrini, V., Bonazzi, D. and DiPietra, A.M. 1991. Analysis of flucytosine dosage forms by derivative UV spectroscopy and liquid chromatography. J. Pharm. Biomed. Anal. 4 : 401-407.
8. Davies, M. A., Schuster, H.F., Brau, J.W. and Meudelsohn, R. 1990. Effects of cholesterol on conformational disorder in dipalmitoylphosphatidylcholine bilayers. A quantitative IR study of the depth dependence. Biochem. 29: 4368-4373.
9. Haris P.I., Robillard, G.T., VanDijk, A.A., and Chapman, D. 1992. Potential of ^{13}C and ^{15}N labeling for studying protein-protein interaction using Fourier transform infrared spectroscopy. Biochem. 31 : 6279-6284.
10. Yung, S.W. 1984. Nuclear Magnetic Resonance Imaging: Basic Principles. pp. 1-164. Rauens Press, New York. N.Y.
11. Derome, A.E. 1987. Modern NMR Techniques For Chemistry Research. Pergamon Press, New York, N.Y. pp. 1-280.
12. Tai, A.W., Lien, E.J., Moore, E.C., Chun, Y., and Roberts, J.D. 1983. Studies of N-hydroxy-N¹-aminoguanidine derivatives by nitrogen-15 nuclear magnetic resonance spectroscopy and as ribonucleotide reductase inhibitors. J. Med. Chem. 16 : 1326-1329.
13. El-Tahtawy, A. and Wolf, W. 1991. In vivo measurements of the intratumoral metabolism, modulation and pharmacokinetics of 5-fluorouracil, using ^{19}F -nuclear magnetic resonances spectroscopy. Cancer Res. 51 : 5806-5812.
14. Karino, K., Kador, P.F., Berkowitz, B. and Balaban, R.S., 1991. ^{19}NMR quantitation of lens aldose reductase activity using 3-deoxy-3-fluoro-D-glucose. J. Biol. Chem. 31 : 20970-20975.
15. Martin, L.F., Peter, A.O., Fehr, D.M., Landis, J.R., Cotter, J., and Briggs, R.W. 1992. ^{31}P -NMR evaluation of postischemia renal ATP and pH levels after ATP-MgCl₂ treatment in rabbits. Am. J. Surg. 164 : 132-139.
16. Bugay, D.E. 1993. Solid-state nuclear magnetic resonance spectroscopy: theory and pharmaceutical applications. Pharm. Res. 10 : 317-327.
17. Harris, K.D.M. and Thomas, J.M. 1991. Probing polymorphism and reactivity in the organic solid state using ^{13}C NMR spectroscopy: Studies of p-formal-trans-cinnamic acid. J. Solid State Chem. 93 : 197-205.
18. Suryananayanan, R. and Wiedmann, T.S. 1990. Quantitation of the relative amounts of anhydrous carbamazepine ($\text{C}_{15}\text{H}_{12}\text{N}_2\text{O}$) and carbamazepine dihydrate ($\text{C}_{15}\text{H}_{12}\text{N}_2\text{O} \cdot 2\text{H}_2\text{O}$) in a mixture by solid-state nuclear magnetic resonance (NMR). Pharm. Res. 7 : 184-187.

19. Jelinski, L.W. 1987. High-resolution NMR of solids. In Dyowski, C. and Lichter, R.L. ed. NMR Spectroscopy Techniques. Marcel Dekker, Inc. New York. PP. 11-253.
20. Reddy, G.P., Chang, C.C., and Bush, C.A. 1993. Determination by heteronuclear NMR spectroscopy of the complete structure of the cell wall polysaccharides of *Streptococcus sanguis* Strin K103. Anal. Chem. 65 : 913-921.
21. Abeygunawardana, C. and Bush, C.A. 1990. Complete structure of the polysaccharide from *Streptococcus sanguis* J22. Biochem. 29 : 2342-2348.
22. Moreau, M., Richards, J.K., and Perry, M. B. 1988. Structural analysis of the specific capsular polysaccharide of *Streptococcus pneumoniae* type 45 American type 72). Biochem. 27 : 6820-6829.
23. Wang, H.P. and Lee, J.S. 1993. Study on the $\Delta^3 \rightarrow \Delta^2$ Isomerization during preparation of cefuroxime double ester prodrugs. J. Food Drug Anal. 1 : 145-153.
24. Nakanishi, K. 1990. One-Dimensional and Two-Dimensional NMR Spectra By Modern Pulse Techniques. University Sciences Books. Mill Valley, California, USA. pp. 1-234.
25. Live, D., Armitage, I.M. and Paterl, D. (eds), 1990. Frontiers of NMR in Molecular Biology. Wiley-Liss, New York, pp. 1-283.

光譜分析法之新應用在生物醫學與藥學分析

連榮吉

美國南加州大學藥學院藥理系

摘 要

近年來許多光譜學在生物醫學與藥學之研究與開發上,已發展為定性與定量之有利工具。它們包括紅外光譜學、核磁共振學、紫外光、可視光譜學及X-射線光譜圖應用於分子結構之判定。本文就其原理介紹並例舉應用實例,包括紅外光譜學、核磁共振學之基本原理、生物醫學上常見之核種(^1H 、 ^2H 、 ^{13}C 、 ^{15}N 、 ^{19}F 、 ^{31}P)之物理性質;利用 ^{13}C 及 ^{15}N 同位素作標飾,以傅氏轉換紅外線光譜儀(FT-IR)作蛋白質與蛋白質相互間之作用研究;利用 ^{15}N NMR決定N-hydroxy-N¹-aminoquanidine衍生物之pKa;利用 ^{19}F -NMR測定3-deoxy-3-F-D

-glucose以定量晶狀體醛糖還原酶之活性;兔子經ATP-MgCl₂處理後,以 ^{31}P -NMR評量腎臟缺血後ATP之量及pH值;利用固態核磁共振儀分析多形體;應用二維核磁共振儀(2D-NMR)作結構判定(COSY、DOFCOSY、NOESY、HMBC、HMQC、2D-INADEQATE);及利用紫外光—可視光微分法分析Flucytosine劑型。

本文希望喚起利用更多之光譜方法,以解決複雜之生物醫學與藥學上之問題。

鍵語:光譜法、紫外光—可視光、X-射線、二維核磁共振、固態核磁共振。